

Electronic Thesis and Dissertation Repository

5-23-2018 1:00 PM

Reactive Oxygen Species and the Regulation of Cerebral Vascular Myogenic Tone

Neil Mazumdar, *The University of Western Ontario*

Supervisor: Welsh, Donald G., *The University of Western Ontario*

A thesis submitted in partial fulfillment of the requirements for the Master of Science degree in Physiology and Pharmacology

© Neil Mazumdar 2018

Follow this and additional works at: <https://ir.lib.uwo.ca/etd>



Part of the [Cellular and Molecular Physiology Commons](#)

Recommended Citation

Mazumdar, Neil, "Reactive Oxygen Species and the Regulation of Cerebral Vascular Myogenic Tone" (2018). *Electronic Thesis and Dissertation Repository*. 5387.
<https://ir.lib.uwo.ca/etd/5387>

This Dissertation/Thesis is brought to you for free and open access by Scholarship@Western. It has been accepted for inclusion in Electronic Thesis and Dissertation Repository by an authorized administrator of Scholarship@Western. For more information, please contact wlsadmin@uwo.ca.

Abstract

The myogenic response refers to the intrinsic ability of arteries to constrict to elevated pressure, developing “tone”. The underlying mechanism has yet to be elucidated but recent evidence suggests that the angiotensin II type 1 receptor (AT1R) is a key mechanosensor, linking intravascular pressure to tone development. One intriguing aspect of this receptor is its ability to activate NADPH oxidase (Nox), an enzyme responsible for the production of reactive oxygen species (ROS). The goal of this study was to ascertain the role of Nox in myogenic tone development. Isolated rat cerebral arteries were mounted in a myograph, pressurized to 60mmHg and diameter measured prior to and following the application of apocynin (a general Nox inhibitor) or ML-171 (a Nox1 specific inhibitor). Pressure-induced constriction was attenuated by apocynin or ML-171 in a concentration dependent manner. This response to ML-171 was attenuated in the presence of paxilline (1 μM) or Ni^{2+} (50 μM), inhibitors of the large-conductance Ca^{2+} -activated potassium (BK_{Ca}) channel and the T-type Ca^{2+} channel $\text{Cav}3.2$, respectively. Control experiments showed no discernable role for Nox2. Subsequent immunohistochemistry confirmed the presence of $\text{Cav}3.2$ and Nox1 in isolated smooth muscle cells, and proximity ligation assay showed the two proteins co-localized within 40nm in the cell membrane. These findings indicate rat arterial Nox1 may regulate the myogenic response by moderating a key negative feedback pathway linked to $\text{Cav}3.2$. This work sheds new light on mechanosensation and how unique signaling proteins impact the ability of resistance arteries to respond to intravascular pressure.

Keywords

NADPH oxidase, reactive oxygen species, myogenic tone, Ca^{2+} channel, large-conductance Ca^{2+} activated potassium channel

Co-Authorship Statement

The quantitative real-time PCR experiments were performed by Frank Visser of the University of Calgary.

Acknowledgements

I would first and foremost like to thank my supervisor Dr. Donald Welsh for accepting me first as a 4th year undergrad student, then a summer student and lab tech, and finally for inviting me to move to London and join your lab as an MSc student. The amount of time and energy you have put into me means a lot. Thank you for your all your guidance and for your patience with me during all of the difficulties I faced up to this point. Your encouragement really helped me get to where I am today.

I would also like to thank the members of my committee, Dr. Qingping Feng, Dr. Rithwik Ramachandran, and Dr. Cristopher Ellis for all your guidance and contributing your ideas to my project.

A big thank you also to Suzanne Welsh, out lab manager, you always keep us on track and kept this entire lab going, it is much appreciated. Thank you to all past and present members of the Welsh lab I have had the pleasure to work with, Ahmed Hashad, Osama Harraz, Maria Sancho, Anil Zechariah, Sergio Fabris, Michelle Kim, Aly Balbaa, William Gao, Hanna Jalali, Rami Alsabbagh, and Claire Linton for all your help with my project and also for all the time spent outside the lab, and just the company and the times when we just got a coffee, you all made my time in the Welsh lab a much better experience.

I would finally like to thank my parents and my sister for their unconditional support this entire time; I am here today because of you.

Table of Contents

Abstract.....	i
Keywords.....	i
Co-Authorship Statement.....	ii
Acknowledgements.....	iii
Table of Contents.....	iv
List of Figures.....	vi
List of Appendices.....	vii
List of Abbreviations.....	viii
1 Introduction.....	1
1.1 The Smooth Muscle Cell.....	2
1.2 Myosin Light-Chain Kinase.....	5
1.3 Myosin Light-Chain Phosphatase.....	5
1.4 The Myogenic Response.....	6
1.5 G-protein Coupled Receptors (GPCRs).....	9
1.6 NADPH Oxidase.....	9
2 Methods.....	14
2.1 Animals, Tissues, and cells.....	15
2.2 Pressure Myography.....	15
2.3 Quantitative real-time PCR.....	16
2.4 Proximity Ligation Assay.....	17
2.5 Immunohistochemistry.....	17
2.6 Chemical, drugs, and enzymes.....	18
2.7 Statistical Analysis.....	18
3 Results.....	19
4 Discussion.....	32
4.1 Background.....	33
4.2 ROS Inhibition and the Myogenic Response.....	34
4.3 Nox Inhibition Dilates Pressurized Arteries.....	35
4.4 Nox1 Impacts BK-mediated Feedback.....	37
4.5 Nox1 Localization with Cav3.2.....	37

4.6 Limitations	40
4.7 Future Directions.....	40
4.8 Summary	41
References	43
Appendices	52
Curriculum Vitae	54

List of Figures

Figure 1: Diagrams of vascular smooth muscle myosin II, MLCK, and MLCP	4
Figure 2: Current understanding of the mechanisms of smooth muscle constriction in the myogenic response.....	8
Figure 3: Nox isoforms found in vascular smooth muscle.	12
Figure 4: Proposed Mechanism of Nox regulation of the myogenic response.....	13
Figure 5: Tissue and mitochondria specific ROS scavenging had no dilatory effect on pressurized rat cerebral arteries.	21
Figure 6: Nox inhibition initiates transient vasodilation.....	22
Figure 7: Nox1 and Nox2 mRNA are expressed in rat cerebral arterial tissue and cells. 23	
Figure 8: Nox1 but not Nox2 inhibition initiates vasodilation.	25
Figure 9: Large-conductance K ⁺ (BK) channel blockade and ML171-induced dilation. 27	
Figure 10: Voltage-gated T-type Calcium Channel (Ca _v 3.2) blockade and ML171-induced dilation.....	28
Figure 11: Nox1 and Cav3.2 localization in rat cerebral vascular smooth muscle cells. .	30
Figure 12: Nox1 and Cav3.2 are found in smooth muscle cells within 40nm of one another.....	31
Figure 13: Proposed Mechanism of Action of Nox1 Regulation of Myogenic Constriction.....	39

List of Appendices

Appendix A: Animal Use Protocol Approval..... 53

List of Abbreviations

AngII	Angiotensin II
AT1R	Angiotensin II type 1 receptor
ATP	Adenosine triphosphate
BK_{Ca}	Large-conductance Ca ²⁺ -activated potassium channel
CaM	Calmodulin
Cav	Voltage-gated Ca ²⁺ channel
DAG	Diacylglycerol
DUOX	Dual oxidase
F actin	Filamentous actin
FAD	Flavin adenine dinucleotide
G actin	Globular actin
GDP	Guanosine diphosphate
GPCR	G-protein coupled receptor
GTP	Guanosine triphosphate
H191	Histidine 191
Ig	Immunoglobulin
IP3	Inositol-1,4,5-triphosphate
KO	Knock out
LC20	Light chain 20

MHC	Myosin heavy chain
MLC20	Myosin light chain 20
MLCK	Myosin light-chain kinase
MLCP	Myosin light-chain phosphatase
MYPT1	Myosin phosphatase targeting subunit 1
NADPH	Reduced nicotinamide adenine dinucleotide phosphate
Nox	Nicotinamide adenine dinucleotide phosphate oxidase
NoxA1	Nox activator 1
NoxO1	Nox organizer 1
p-LC20	Phosphorylated light chain 20
PKC	Protein kinase C
PLA	Proximity ligation assay
PLC	Phospholipase C
PolDIP	Polymerase delta interacting protein
PP1c-δ	Protein phosphatase 1c delta
ROK	Rho kinase
ROS	Reactive oxygen species
RyR	Ryanodine receptor
SR	Sarcoplasmic reticulum
STOC	Spontaneous transient outward current

T697	Threonine 697
T855	Threonine 855
TPP+	Triphenylphosphonium
TRP	Transient receptor potential
VGCC	Voltage-gated Ca ²⁺ channel

1 Introduction

The cardiovascular system is comprised of a muscular pump and a network of arteries, veins, and capillaries which transport blood throughout the body. The major types of arteries include larger conduit vessels such as the aorta, and smaller resistance vessels, which include the vascular beds that permeate the organs. Larger vessels are not considered to be able to dynamically control blood flow, while the resistance arteries are known to respond to a variety of stimuli including blood flow, tissue metabolism, and intraluminal pressure (1-4) to actively change diameter in order to regulate the magnitude and distribution of blood flow to the organs. This process is controlled by arterial smooth muscle contraction, which in turn is governed by the phosphorylation state of the myosin light chain 20 (LC20) via the opposing activities of myosin light chain kinase (MLCK) and myosin light chain phosphatase (MLCP) (5)

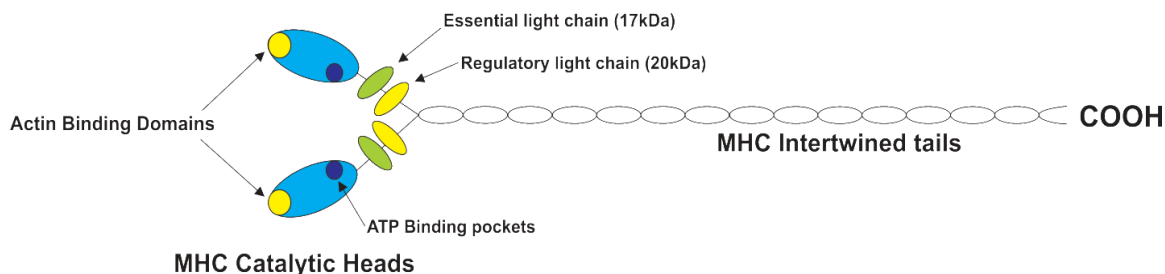
1.1 The Smooth Muscle Cell

Arteries are comprised of two main cell types; endothelial and smooth muscle. The innermost layer of the artery is made of a single layer of endothelial cells arranged longitudinally along the vessel. Outside this are ~1-3 layers of smooth muscle cells wrapped circumferentially around the vessel (6,7). The two cell types are separated by an internal elastic lamina. Smooth muscle cells have an elongated structure with tapered ends and a single nucleus. They are comprised of two types of fibres: the thick filament myosin, and the thin filament actin. The filaments run parallel to one another throughout the cell and are anchored at sites termed focal adhesions, which also contain membrane-spanning proteins known as integrins (5,8). Smooth muscle type II myosin is the specific myosin isoform accepted to be responsible for force generation in vascular smooth muscle cells (5). Each myosin molecule consists of two myosin heavy chain (MHC) amino acid sequences coiled around one another in a double-helix to form a “tail” region (Figure 1A). Globular enzymatic heads containing actin binding domains are found at the N-terminus of the sequences. They are connected to the tail regions by a neck region, which consists of a 20-kilodalton (kDa) regulatory light chain (LC20) and a 17-kDa essential light chain (5) (Figure 1A).

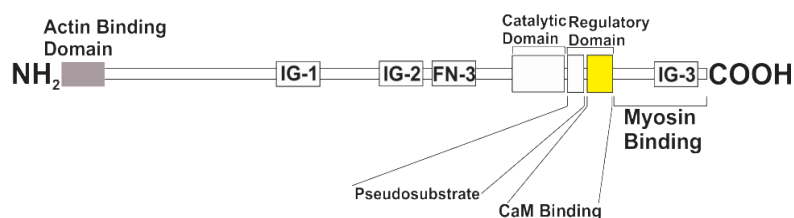
Actin is the most abundant protein in smooth muscle. It is made up of individual 42-kilodalton monomers which can exist as single units termed globular (G) actin, or as

polymers made of multiple subunits forming filamentous (F) actin (5,8,9). Actin filaments are anchored at the cell membrane at focal adhesions, and to one another in the cytosol at dense bodies (8). Muscle contraction occurs due to the interaction of actin filaments with myosin, a process regulated by the reversible phosphorylation of myosin LC20 at the serine 19 (S-19) site. Phosphorylated LC20 (p-LC20) allows actin to activate MgATPase to use energy from adenosine triphosphate (ATP) to bind the myosin head domain to actin (5). There is a subsequent movement of the myosin heads, termed a “power stroke”, and the actin filaments slide toward the focal adhesions, which results in the shortening of muscle fibres, and ultimately muscle contraction (5,8,9). The phosphorylation of LC20 is therefore critical in muscle contraction and is regulated by the opposing activities of MLCK and MLCP (5).

A Smooth Muscle Myosin II



B MLCK



C MLCP



Figure 1: Diagrams of vascular smooth muscle myosin II, MLCK, and MLCP (A): Diagram of vascular smooth muscle myosin II containing two catalytic heads containing actin and ATP binding regions connected to two intertwined myosin heavy chain tails. The neck region connects the heads and tails and contains an essential light chain and a regulatory light chain which is the site of phosphorylation required for contraction. **(B):** Myosin light chain kinase is an elongated protein with an N-terminal actin binding region and a C-terminal myosin binding region. A regulatory domain consists of a pseudosubstrate and $(Ca^{2+})_4CaM$ binding site which unfolds the pseudosubstrate, allowing the adjacent catalytic site to phosphorylate LC20. **(C)** Myosin light-chain phosphatase is an elongated protein containing N-terminal PP1c- δ phosphatase which binds to the MYPT1 subunit via an RVxF when the protein is active. Adjacent ankyrin repeats are thought to facilitate the interaction among proteins. MYPT1 activity is modulated via two phosphorylation sites; threonine (T) 697 and T855. The function of the C-terminal M20 subunit is not known (5).

1.2 Myosin Light-Chain Kinase

Smooth muscle MLCK is a 125-kDa elongated protein. It consists of an N-terminus actin binding domain, a coiled PEVK repeat, three immunoglobulin (Ig) domains, and a fibronectin (Fn3) and C-terminal catalytic, regulatory, and calmodulin (CaM) binding domains (5) (Figure 1B). Also near the C-terminus is the autoinhibitory pseudosubstrate, which is folded over the catalytic domain when MLCK is in its inactive state, preventing access to myosin LC20 (5). Activation of MLCK requires the entry of calcium into the cytosol, which occurs through voltage gated L-type Ca channels in smooth muscle (4) (Figure 1B). The intracellular calcium binds to the protein CaM, creating a $(Ca^{2+})_4CaM$ complex which unfolds the autoinhibitory substrate exposing the catalytic domain. This allows the catalytic domain to phosphorylate LC20 via activity of phosphotransferase. Only one of two myosin heads requires phosphorylation, and subsequently is bound to actin, forming an actin-myosin crossbridge. The myosin head can then move pulling actin along with it in a “power stroke” resulting in the shortening of muscle fibres, leading to vessel constriction (5).

1.3 Myosin Light-Chain Phosphatase

Smooth muscle MLCP consists of three major domains; a ~38 kDa catalytic subunit protein phosphatase 1c-delta (PP1c- δ), a ~110-130 kDa myosin-targeting subunit (MYPT1), and a ~20 kDa subunit of unknown function (Figure 1C). Its well-established role is to counterbalance MLCK activity and attenuate constriction by dephosphorylating LC20 (5, 12). This is achieved via activity of the PP1c- δ phosphatase, while the MYPT1 subunit confers specificity of PP1c- δ to LC20 (5, 12). Regulation of the MYPT1 subunit is of particular interest due to its essential role of targeting of LC20 for dephosphorylation. A well-established mechanism of MYPT1 regulation is via phosphorylation at its threonine 855 (T855) or T697 sites, which prevents MYPT1 from targeting PP1c- δ to p-LC20 thereby allowing sustained contraction. Studies have shown phosphorylation of MYPT1 at either its T855 or T697 site have increased smooth muscle contraction (5, 12). This process is governed through RhoA activation in response to a contractile stimulus. RhoA subsequently activates Rho kinase (ROK) which is responsible for MYPT1 phosphorylation. The regulation of vascular smooth muscle

contraction is required in resistance vessels in order to tightly regulate the magnitude and distribution of blood flow to the organs. It can be viewed as regulation of the opposing activities of MLCK and MLCP, but both these processes require an upstream stimulus in order for activation. Several such stimuli exist, including blood flow, tissue metabolism, (1-4) and intravascular pressure.

1.4 The Myogenic Response

Over a century ago, Bayliss first surmised that arteries could respond to a fluctuating change in blood pressure. The so-called “myogenic response” has been widely observed and is prominent in the cerebral vasculature where constant perfusion must be maintained over a range of blood pressures (13). It is critical, therefore, that the mechanisms that tightly regulate tone are understood, as they may be useful for developing therapeutic targets. The work of Knot & Nelson established that voltage-gated long lasting, or L-type, calcium channels play a critical role in the myogenic response (4). Intravascular pressure activates mechanosensitive cation channels, resulting in depolarization which in turn increases the activity of L-type channels and provides the intracellular calcium required for vessel constriction. This response is typically assessed with pressure myography, a technique in which arterial segments are isolated, cannulated at each end and attached to a pressure pump to control intraluminal pressure. The vessel is bathed in circulating physiological salt solution and its diameter measured using a microscope and automated edge detection software.

Classically, pressure-induced changes in arterial tone have been ascribed to a three-step process. First, a membrane bound mechanosensor will sense pressure, leading to the activation of a signalling pathway which activates downstream targets that ultimately result in tone development. The primary signalling mechanisms that regulate myogenic tone involve regulating the phosphorylation of LC20 either through activation of MLCK or inhibition of MLCP (5). Some studies suggest that pressure activates mechanosensitive non-selective cation channels, namely the transient receptor potential (TRP) channels (5, 8, 14), whose activity depolarizes the cell, increasing activity of L-type Ca^{2+} channels. The resulting influx of Ca^{2+} results in CaM binding and subsequent activation of MLCK, which acts to phosphorylate LC20 (Figure 1). Additionally, intravascular pressure is

thought to activate RhoA GTP, resulting in ROK-induced phosphorylation of the MYPT1 subunit, which inhibits MLCP activity (5, 15-17). Recent studies have also suggested that cytoskeletal dynamics (i.e. the conversion of globular (G) to filamentous (F) actin), are involved in tone regulation (9, 19, 20).

One question of great interest is the identity of the receptor or sensor that activates downstream targets inducing myogenic constriction. Two of the main candidates include integrins and G-protein coupled receptors (8, 21-25) however there is no general agreement as to which one regulates myogenic response. Integrins are membrane spanning proteins found at focal adhesions which link the actin cytoskeleton to the extracellular matrix, and thereby transduce force (8, 26). Integrin specific blockade has been shown to attenuate tone in pressurized vessels (26). Finally, the candidate that has been more recently investigated is the family of G-protein coupled receptors (21). Recent evidence suggests that in addition to acting through classic G-protein signalling cascades, these receptors can also act as mechanosensors to trigger myogenic constriction (21-23); this formed the basis of the present study. Specifically, recent findings suggest that the angiotensin type one receptor (AT1R), a classic G_q coupled protein receptor may be mechanosensitive and induce constriction (21-23).

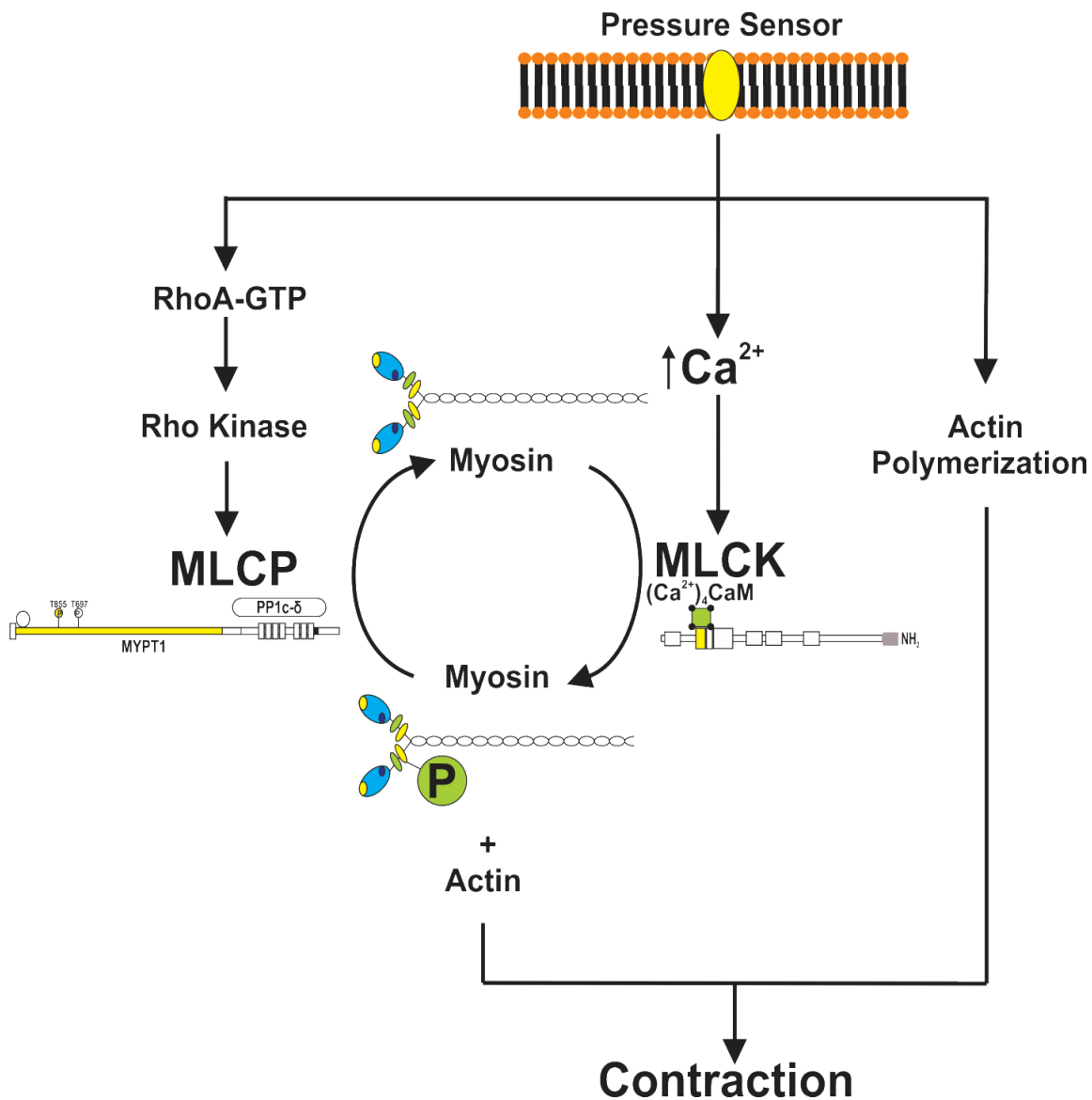


Figure 2: Current understanding of the mechanisms of smooth muscle constriction in the myogenic response. An unknown plasma membrane sensor activates downstream signalling pathways, resulting in increased activity of MLCK or inhibition of MLCP, both of which result in enhanced phosphorylation of MLC20 leading to constriction. The polymerization of actin has also been suggested to enhance constriction (9, 19, 20).

1.5 G-protein Coupled Receptors (GPCRs)

GPCRs are the largest family of membrane bound proteins and regulate a wide variety of physiological functions. These proteins generally consist of seven segment membrane-spanning receptors bound to a cytosolic G-protein. Broadly speaking, they are activated by a ligand binding to a binding pocket on the receptor, causing a conformational change which subsequently activates the G-protein which can then signal further downstream targets (27). GPCRs are divided into five families: rhodopsin (A), secretin (B), glutamate (C), adhesion (D), and frizzled/taste (E) (28, 29). These are further divided into multiple subfamilies based on differences in G-protein subtypes and signalling pathways. Recent work has suggested that GPCRs, in particular the Angiotensin II type-1 receptor (AT1R) of the rhodopsin family (29) can sense intravascular pressure, initiating downstream signalling pathways resulting in constriction (21-23). Angiotensin II (Ang II) is a well-established vasoconstrictor that acts with the AT1R in a classic G-protein coupled receptor mechanism (30, 31). Binding of AngII to the AT1R activates Phospholipase C (PLC), producing Inositol 1,4,5-triphosphate (IP3) and diacylglycerol (DAG). IP3 causes the release of Ca^{2+} from the sarcoplasmic reticulum (SR) whereas DAG will induce arterial depolarization. Both events will increase cytosolic $[\text{Ca}^{2+}]$, subsequently mobilizing calmodulin. The Ca^{2+} -calmodulin complex then binds to and activates MLCK resulting in LC20 phosphorylation and constriction (30- 32). AT1R is also known to induce contraction by increasing RhoA activity, which in turn increases ROK-induced phosphorylation of the MYPT1 subunit of MLCP, thereby reducing its ability to dephosphorylate LC20 (31, 33). The AT1R has other downstream targets in vascular smooth muscle which may play a role in the myogenic response. Of particular interest is the reactive oxygen species (ROS) generating enzyme, termed the nicotinamide adenine dinucleotide phosphatase (NADPH) oxidase (Nox) (32).

1.6 NADPH Oxidase

In addition to the well-known agonist induced constriction pathway, AT1R activation has also been shown to stimulate the reduced Nox enzyme in cerebral vasculature (32), whose function is to form reactive oxygen species (ROS) via the transfer of electrons from NADPH to oxygen molecules. The Nox family of enzymes consists of seven

isoforms: Nox1-5, dual oxidase (DUOX) 1, and DUOX 2. Nox1, 2, 4, and 5 expression has been confirmed in the cerebral vasculature (34). Upon activation, a catalytic subunit transfers electrons in succession from the NADPH substrate to flavin adenine dinucleotide (FAD), and then to two iron atoms located within its membrane-bound subunit, and finally to extracellular oxygen, forming the superoxide anion O_2^- (32, 34-36) (Figure 3). The superoxide anion is the parent molecule that can form other ROS (32, 34-36). In the cerebral vasculature, O_2^- can react with superoxide dismutase (SOD) to form hydrogen peroxide (H_2O_2), or with endothelial nitric oxide (NO) to prevent its relaxing effect and instead produce $ONOO^-$, a highly reactive compound (34-36).

The first isoform to be discovered was Nox2, also called gp91phox, (phagocyte oxidase) as it was originally found in phagocytes (35, 36). Nox2 is a catalytic subunit comprised of six transmembrane α -helices bound to the subunit p22phox to form an inactive enzyme complex at the cell membrane. The Nox2 subunit binds 2 heme molecules containing iron and one FAD molecule, a cofactor of NADPH. The G-protein Rac is also bound to the catalytic subunit, and is believed to be essential in Nox activation by exchanging guanosine triphosphate (GTP) for guanosine diphosphate form (GDP), which allows it to catalyze the electron transfer from NADPH to FAD (37). Also required for Nox activation are the subunits, p47phox, and p67phox, which form a cytosolic complex along with p40phox. Nox activation requires phosphorylation of p47phox by protein kinase C (PKC) or tyrosine kinases (Src) which causes the cytosolic complex to translocate to the membrane and bind the Nox catalytic subunit. Next, p67phox is believed to be crucial in stimulating the electron transfer from NADPH (35, 36, 38). Nox1 structure and function is very similar to that of Nox2. It contains a catalytic subunit and p22Phox, forming a membrane bound complex as well as a cytosolic complex which, in vascular tissue, must translocate to the membrane in order to induce enzyme activity (35, 36, 38). Nox1 is most highly expressed in colon cells, and here, the cytosolic complex is composed of Nox organizer 1 (NoxO1) and Nox activator 1 (NoxA1), which are considered homologues of p47phox and p67phox respectively (34-36, 38). Unlike p47phox, NoxO1 is constitutively active, increasing Nox1 activity and producing ROS. While vascular smooth muscle Nox1 does contain NoxA1 in place of p67phox, it is similar to Nox2 in that it contains p47phox rather than NoxO1, and requires

phosphorylation for Nox activation (35, 36, 38). Figure 3 is a schematic of the various Nox isoforms.

Nox4, while originally discovered in kidney cortex, is also present in human and rodent vascular smooth muscle cells. Similarly to Nox1/2, it contains a membrane bound complex consisting of the Nox catalytic subunit containing heme molecules and FAD, and p22phox (35, 36). Nox4 is constitutively active without the presence of a cytosolic complex, and its activity can be increased by binding of polymerase delta interacting protein (PolDIP) 2 to p22phox (35, 36, 38). Nox5 on the other hand is not regulated by additional subunits but contains an EF hand motif which acts as a Ca^{2+} binding domain, and its activity is regulated by Ca^{2+} and CaM. Current evidence suggests that Nox1 and 2 are the isoforms most dominant in vascular smooth muscle, while Nox4 is expressed primarily in endothelial cells and Nox5 expression has been confirmed in humans but not rodents (36, 38). This study will therefore focus primarily on Nox1 and Nox2.

Nox-generated ROS may potentially facilitate myogenic constriction through regulation of L-channels (10, 11) or moderate tone by regulating feedback mechanisms (5). These feedback mechanisms generally involve depolarization-activated potassium channels such as voltage gated potassium (K_v) channels or large-conductance calcium activated potassium (BK_{Ca}) channels which hyperpolarize cells, and lowering L-type Ca^{2+} channel activity (10, 11). The well-established BK mediated negative feedback pathway on the myogenic response requires BK_{Ca} channel activation via Ca^{2+} which is provided by ryanodine receptors (RyR) located on the sarcoplasmic reticulum (SR). BK_{Ca} activity then results in cell hyperpolarization, lowering L-channel activity, thereby attenuating constriction (10, 11, 39). Although evidence exists that ROS can enhance the activity both of L- and T-type Ca^{2+} channels (40, 41), the role of ROS in facilitating myogenic tone has not been studied. This will be the focus of the present study.

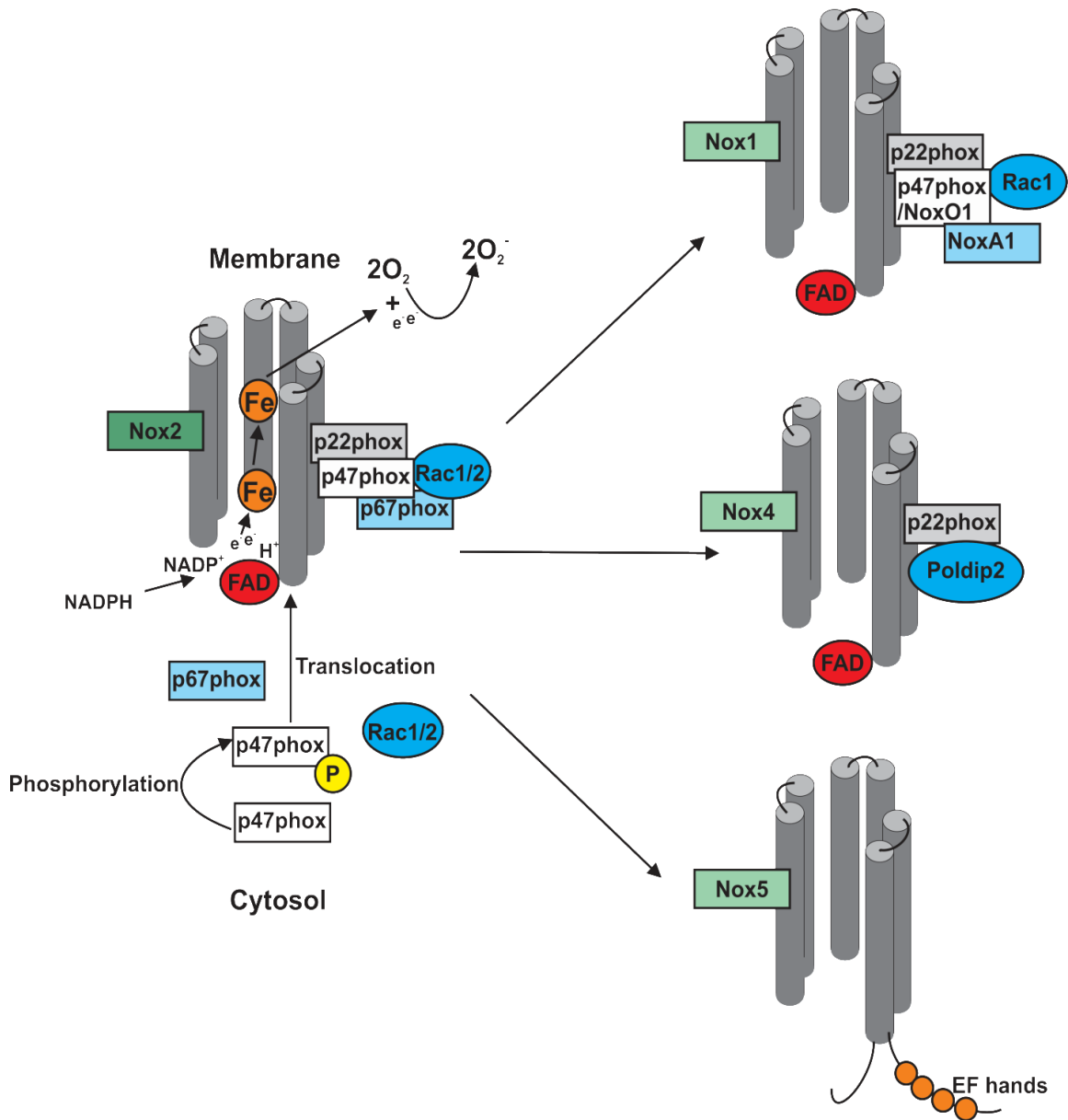


Figure 3: Nox isoforms found in vascular smooth muscle. Nox2 is considered the classic prototype, while Nox 1, 4, and 5 are the other isoforms found in vascular myocytes. It contains a membrane subunit bound to p22phox. Activation requires phosphorylation of the cytosolic p47phox, which then translocates to the membrane, binding to p22phox, causing binding of additional subunits p67phox and Rac. Similar to Nox2, Nox1 activation also requires phosphorylation of a cytosolic subunit (NoxO1 in colon or p47phox in the vasculature) in order for cytosolic components to translocate to the membrane. Nox4 activity is upregulated by polymerase delta interacting protein (PolDIP)2 while Nox5 requires no additional subunits but is activated by Ca^{2+} binding to its EF-hand motif.

1.7 Goals and Hypothesis

Goal: to determine the role played by Nox enzymes in regulating myogenic tone in cerebral arteries. Two specific aims are forwarded:

Specific aim 1: Determine the impact of Nox enzymes in the regulation of myogenic tone.

We hypothesize that vascular smooth muscle Nox activity facilitates myogenic constriction

Specific aim 2: Determine the mechanism linking Nox to myogenic tone.

We hypothesize that vascular smooth muscle Nox facilitates myogenic constriction by inhibiting the T-type calcium channel, resulting in less BK channel activity, ultimately inhibiting the feedback response on myogenic tone.

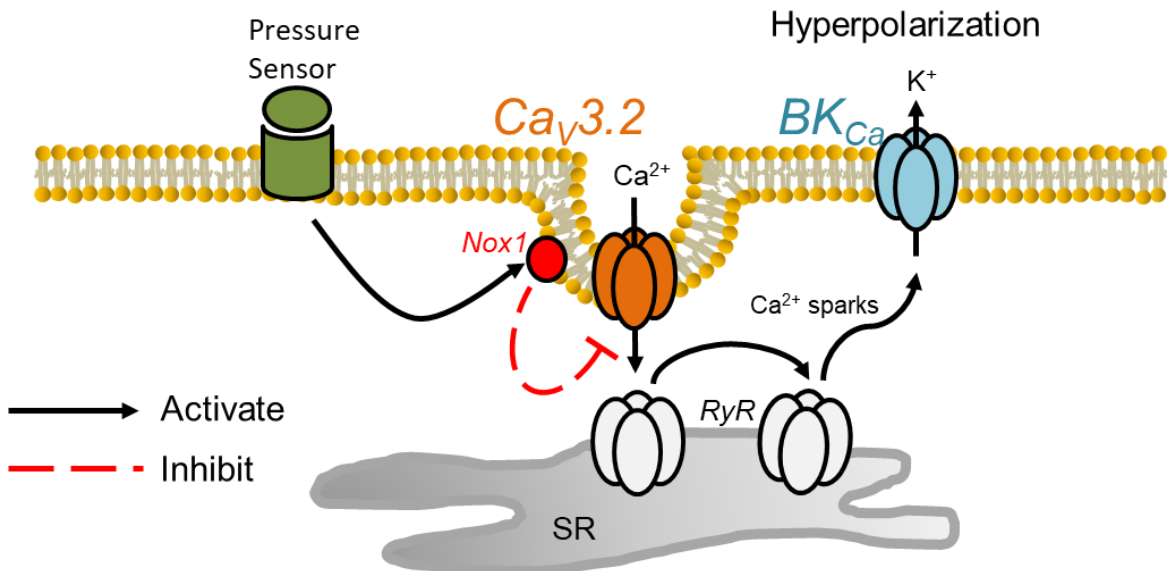


Figure 4: Proposed Mechanism of Nox regulation of the myogenic response. A pressure sensor activates Nox, which inhibits Cav3.2, resulting in the reduction of Ca²⁺ sparks and subsequently reduced spontaneous transient outward current (STOC) production from the BK channel and attenuated hyperpolarization, allowing L-type channels to remain active, facilitating constriction.

2 Methods

2.1 Animals, Tissues, and cells

All procedures were approved by the University of Western Ontario Animal Care Committee. Female Sprague-Dawley rats were euthanized via carbon dioxide asphyxiation. The brain was gently removed and placed in ice-cold phosphate buffered saline solution (PBS) (pH 7.4) containing (mM) 138 NaCl, 3 KCl, 10 Na₂HPO₄, 2 NaH₂PO₄, 5 glucose, 0.1 CaCl₂, and 0.1 MgSO₂. Third order posterior cerebral arteries were dissected and cut into 2-3 mm segments and stored in PBS to be used the same-day for pressure myography, PCR or enzymatic digestion.

Smooth muscle cells from rat arteries were enzymatically isolated as previously described (11). Briefly, arterial segments were placed in an isolation medium (37°C, 10 min) containing (in mM): 60 NaCl, 80 Na-glutamate, 5 KCl, 2 MgCl₂, 10 glucose and 10 HEPES with 1 mg/ml bovine serum albumin (pH 7.4). Vessels were then exposed to a two-step digestion process that involved: 1) 12-15 min incubation in isolation medium (37°C) containing 0.5 mg/ml papain and 1.5 mg/ml dithioerythritol; and 2) a 15 minutes incubation in isolation medium containing 100 µM Ca²⁺, 0.7 mg/ml type F collagenase and 0.4 mg/ml type H collagenase. Endothelial cells were similarly isolated using the following digestion process: 1) a 30-min incubation in isolation medium (37°C) containing 1mg/mL BSA, 100 µM Ca²⁺, 1 mg/mL papain and 1 mg/mL dithioerythritol; and 2) a 10-min incubation in isolation medium containing 1mg/mL BSA, 100 µM Ca²⁺, 0.9 mg/mL type-F collagenase, 0.6 mg/mL type-H collagenase, 5 mg/mL elastase and 1 mg/mL trypsin inhibitor. Following incubation, tissues were washed repeatedly with ice-cold isolation medium and triturated with a fire-polished pipette. Liberated cells were manually picked with a suction pipette and stored in ice-cold isolation medium for use the same day within ~5 hr.

2.2 Pressure Myography

Cerebral arteries were cannulated on a pressure arteriograph and superfused in 37°C physiological saline solution (PSS) of pH 7.4 containing 119 mM NaCl, 4.7 mM KCl, 20 mM NaHCO₃, 1.1 mM KH₂PO₄, 10 mM glucose, 1.6 mM CaCl₂, and 1.2 mM MgSO₄ while in a bath of Ca²⁺-free PSS (10). Artery diameter was measured using pressure

myography techniques adapted from Abd El-Rahman et al (10). Briefly, arteries were initially pressurized to a baseline of 15mmHg and given an initial equilibration period (~25 min) in Ca²⁺-free PSS, followed by a second equilibration period (~10 min) in PSS Ca²⁺, at which time vessel viability was tested by applying 55 mM external K⁺. Vessels were considered viable if they constricted to ~50% of their initial baseline diameter in response to K⁺ and returned to baseline following wash off in PSS. A pressure stimulus of 60mmHg was applied until stable myogenic constriction was achieved (~5 minutes). The vessel was returned to 15mmHg (10 min) and pressure increased to 60mmHg to stimulate myogenic tone and held at this pressure for the duration of the experiment. Diameter was measured after ten minutes at 60mmHg under control conditions with no added reagents and under experimental conditions with the addition of pharmacological inhibitors of ROS. Next, 200 nM nifedipine was applied (5 min), followed by 2 mM EGTA to determine passive vessel diameter.

2.3 Quantitative real-time PCR

Quantitative real-time PCR was performed as previously described (10, 11). Briefly, smooth muscle (~200) and endothelial cells (~100) were isolated from middle cerebral arteries (n=4 arteries/group) and whole middle cerebral arteries (~2 from n=4 arteries/group) and placed in RNase- and DNase-free collection tubes. Total RNA was extracted (RNeasy plus micro kit Qiagen, USA) and first-strand cDNA synthesized using the Quantitect reverse transcription kit (Qiagen) according to instructions. For the negative control groups, all components except the reverse transcriptase were included in the reaction mixtures. Q-PCR was performed using the Kapa SYBR Fast Universal qPCR Kit (Kapa Biosystems). Rat beta actin (ACTB) gene was utilized as the reference gene. Control reactions and those containing cDNA from cerebral arteries were performed with 1 ng of template per reaction. Due to the very small quantities of RNA obtained from isolated smooth muscle cells (~200 cells), the entire cDNA yield from each preparation was used to assay the full set of test and housekeeping genes. The running protocol included 45 cycles consisting of 95°C for 5 s, 55°C for 15 s, and 72°C for 10 s using an Eppendorf Realplex 4 Mastercycler. PCR specificity was checked by dissociation curve analysis. Assay validation was confirmed by testing serial dilutions of pooled template

cDNAs suggesting a linear dynamic range of 0.1–100 ng template and yielded percent efficiencies ranging from 85 to 108%. Template controls did not yield detectable fluorescence. Expression of the Nox1 or Nox2 isoforms in cerebral arteries, endothelial, or smooth muscle cells (n=4 arteries/ group) relative to control tissue was determined using the relative expression software tool (REST) version 2.0.13.23. The primers for RT-qPCR were as follows:

Nox1: TCAAACAGAAGAGAGCATGAGTG and CGAGGATCCACTTCCAAGAC

Nox2: TGTGTCGGAATCTCCTCTCC and CCGTGTGAAGTGCTATCATCC.

Actin: AGCACCCCTGTGCTGCTCAC and GTACATGGCTGGGGTGTTG.

2.4 Proximity Ligation Assay

The Duolink in situ PLA kit was used for proximity ligation assay. Isolated vascular smooth muscle cells were fixed in PBS containing 4% paraformaldehyde (15 min), permeabilized in PBS containing 0.2% Tween20 (15 min). Cells were then washed with PBS, blocked in Duolink blocking solution (1 h, 37°C), and incubated overnight (4°C) with primary antibodies (rabbit anti-Cav3.2 and rabbit anti-Nox1) in Duolink antibody diluent solution. Cells were labelled with Duolink PLA PLUS and MINUS probes (1 h, 37°C). The secondary antibodies of PLA PLUS and MINUS probes are attached to synthetic oligonucleotides that hybridize when in close proximity (<40 nm). The hybridized oligonucleotides were then ligated using Duolink ligase (30 min, 37°C) prior to rolling circle amplification with Duolink polymerase (90 min, 37°C). The amplification products extending from the oligonucleotide arm of the PLA probes were detected using red fluorescent fluorophore-tagged, complementary oligonucleotide sequences and a Leica-TSC SP8 confocal microscope.

2.5 Immunohistochemistry

Rat smooth muscle cells were enzymatically isolated as described above. Cells were fixed in 4% paraformaldehyde for (15 min, room temperature) and permeabilized in PBS containing 0.2% Tween20 for 15 min (room temperature). Cells were blocked using PBS with 0.2% Tween20 and either 3% goat serum for Nox1, or 3% donkey serum for

Cav3.2. Cells were incubated overnight at 4°C with primary antibodies against smooth muscle Cav3.2 (1:100 dilution), and Nox1 (1:100 dilution), in working solution (0.2% Tween20 in PBS with 2% donkey serum for Cav3.2 or 2% goat serum for Nox 1). Next, cells were washed 4 times with PBS (5 min each, 22°C) and incubated with working PBS solutions containing secondary antibodies (1h, 22°C). Following washes with PBS, coverslips containing cells were mounted on glass slides containing mounting media and stored (4°C). Controls were obtained by omitting the primary antibody. All reactions involved the use of fluorophore-conjugated secondary antibodies (1:200 dilution): Alexa Fluor 488-donkey anti-rabbit IgG, and Alexa Fluor 633-goat anti-rabbit IgG. Immunolabelling was assessed using a Leica-TSC SP8 confocal microscope.

2.6 Chemical, drugs, and enzymes

The proximity ligation kit was purchased from Duolink. Buffer reagents, collagenases (types F and H), dithioerythritol, paxilline, and mitoTEMPO were purchased from Sigma-Aldrich. Papain and elastase were acquired from Worthington (USA) and Calbiochem (USA), respectively. TEMPOL, ML-171, and apocynin were purchased from Tocris, gp91-ds-tat was purchased from AnaSpec

2.7 Statistical Analysis

Data was expressed as means \pm SE and n indicates the number of vessels or cells. For vessel diameter measurements, data was also expressed in box-and-whisker plots. One-way repeated measures ANOVA and paired t-tests with Bonferroni post-hoc tests were performed as needed on vessels or cells to compare the effects of a given condition/treatment on arterial diameter. (Sigmaplot, SPSS). P values ≤ 0.05 were considered statistically significant.

3 Results

To begin assessing the effects of ROS on the blood vessel regulation, we ascertained the impact of a general scavenger (TEMPOL) on myogenic tone by sequentially increasing its concentration in the bath with rat cerebral arteries pressurized to 60 mmHg. Figure 5A & 5B highlight the presence of a strong myogenic response yet the absence of a dilatory or constrictor effect of TEMPOL as bath concentration rose from 10 to 100 μ M. This result was surprising but TEMPOL is known to have broad scavenging effects; we rationalized that this superoxide dismutase mimetic might be simultaneously mitigating ROS dependent mechanisms that are dilatory and constrictive. We repeated the preceding experiment with target-selective agents, starting with MitoTEMPO, an agent that selectively scavenges mitochondria-derived ROS. Analogous to the preceding findings, MitoTEMPO, at concentrations ranging from 1 to 30 μ M had no substantive impact on myogenic tone development (Figure 5C & 5D).

The Nox family of enzymes are another rich source of ROS in the vasculature whose activity has been linked to tone development (30-32, 40-42). To study their effect on cerebral arterial myogenic tone development, myography experiments were performed in the absence and presence of apocynin, a broad Nox inhibitor whose bath concentration was sequentially increased from 30-300 μ M. Working in endothelial intact and denuded preparations, the latter condition induced by passing an air bubble down the lumen, apocynin was observed to induce a transient concentration-dependent dilation over the first 120 seconds followed by a slower constriction, with vessels returning modestly close to baseline within ten minutes (Figure 6). While this data indicate a role for Nox in facilitating the myogenic response, the isoform responsible for this effect remained unclear. In this regard, real-time PCR analysis was performed focusing on Nox1 and Nox2, the two dominant isoforms found in vascular tissue (Figure 7) (34-36, 38). Consistent with the literature, we observed mRNA product for Nox1 and Nox2 in whole cerebral arteries (34) (Figure 7A). Likewise, both isoforms were observed at the mRNA level in freshly isolated smooth muscle and endothelial cells, roughly in equally proportion. (Figure 7 B&C).

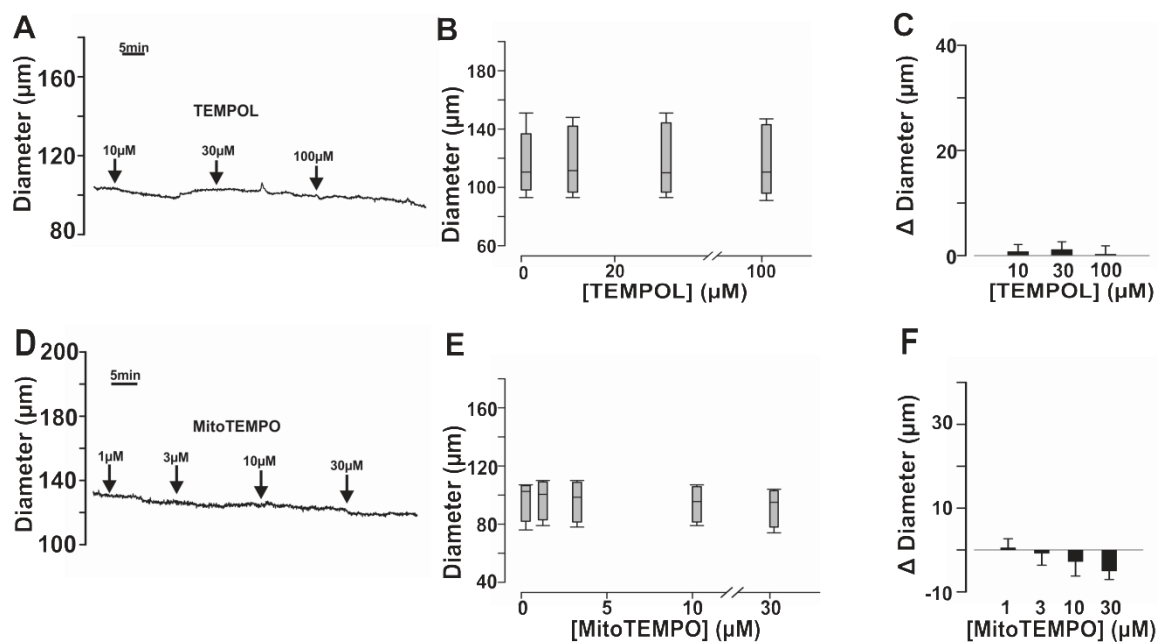


Figure 5: Tissue and mitochondria specific ROS scavenging had no dilatory effect on pressurized rat cerebral arteries. (A, D) Representative traces documenting the effects of TEMPOL (A) or MitoTEMPO (D) on vessel diameter. (B, E) Summary data of vessel responsiveness (n=6 vessels from 6 animals) to TEMPOL (B: 10-100 µM) or MitoTEMPO (E: 1-30 µM). (C, F) maximum change in diameter from each concentration of TEMPOL (C) or MitoTEMPO (F) relative to control.

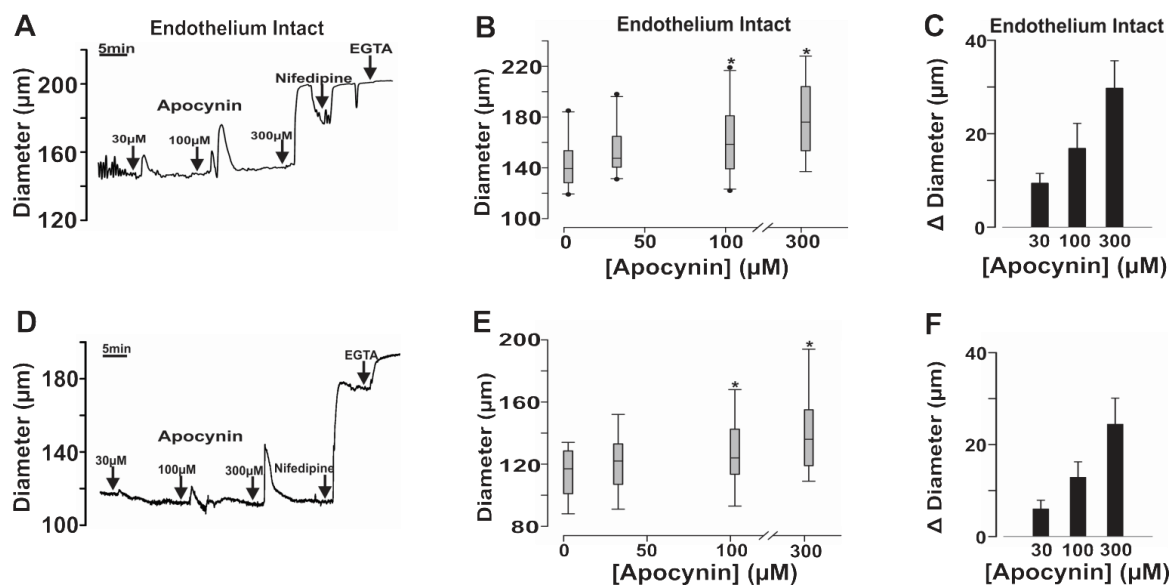


Figure 6: Nox inhibition initiates transient vasodilation. (A, D) Representative traces documenting the effects of Nox inhibition (Apocynin) in endothelium intact (A) and denuded (D) vessels. (B, E) Summary data of vessel responsiveness ($n=6$ vessels from 6 animals) to apocynin (30-300 μM) in endothelium intact (B) and denuded vessels (E). (C, F) Maximum change in diameter from each concentration of apocynin in endothelium intact (C) or denuded (F) vessels relative to control. * Indicates significant difference from control; repeated measures ANOVA and Bonferroni post-hoc analysis.

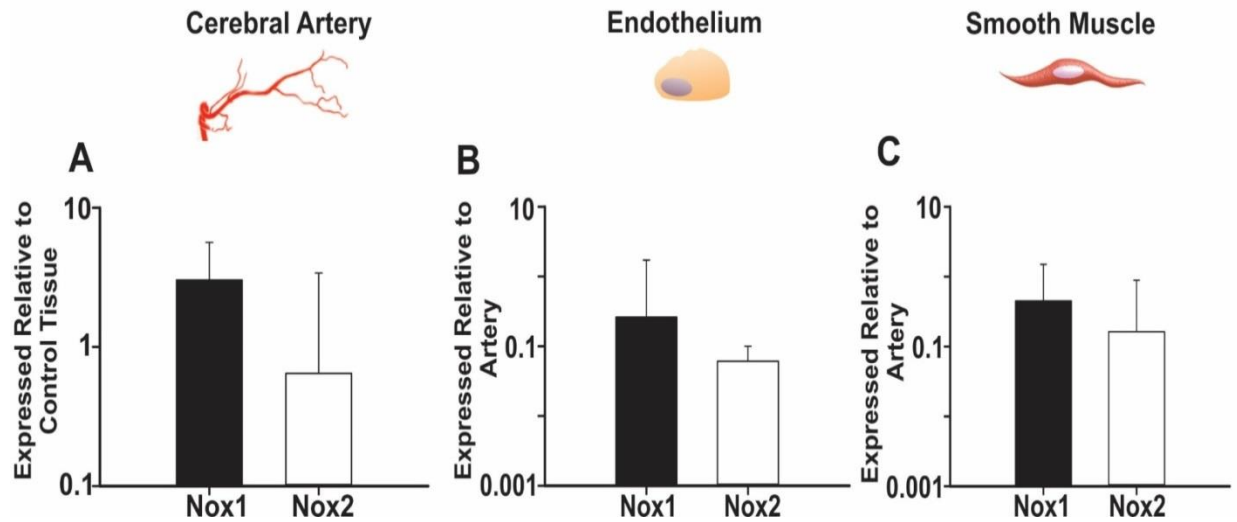


Figure 7: Nox1 and Nox2 mRNA are expressed in rat cerebral arterial tissue and cells. (A) Real-time PCR data showing Nox1 and Nox2 mRNA expression in cerebral arteries (n=4 arteries) relative to rat ileum and lung, respectively. (B-C) Nox1 and Nox2 mRNA expression in endothelial (n~100 cells from 4 arteries) (B) and smooth muscle (n~200 cells from 4 arteries) (C) cells expressed relative to whole arterial tissue.

Having confirmed the presence of Nox1 and Nox2 at the mRNA level, we next studied their involvement in myogenic tone development. We performed pressure myography on endothelium denuded vessels pressurized to 60mmHg and bathed in a Nox1-specific (ML171, 1 to 30 μ M) or Nox2 specific (gp91-dstat, 0.5 to 10 μ M) inhibitor. The application of ML-171 induced, in a concentration dependent manner a transient dilation in rat cerebral arteries within the first two minutes, followed by a slower and incomplete return to baseline (Figure 8A & 8B). In contrast, Nox2 inhibition by gp91-dstat had no substantive impact on vessel diameter irrespective of the bath concentration (Figure 8C & 8D). Taken together, the preceding data support Nox1 rather than Nox2 aiding in the development of myogenic tone in rat cerebral circulation.

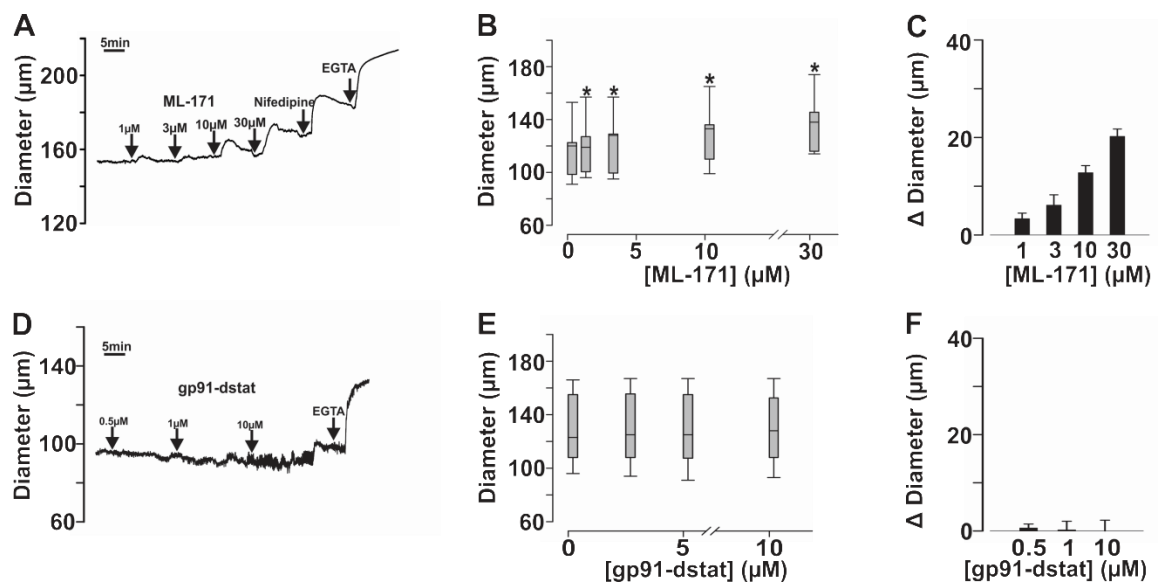


Figure 8: Nox1 but not Nox2 inhibition initiates vasodilation. (A, D) Representative traces documenting the effects of Nox1 (ML-171) (A) or Nox2 inhibition (gp91-dstat) (D). (B, E) Summary data of vessel responsiveness to ML-171 (n=9 vessels from 9 animals) (B; 1-30 μM) or gp91-dstat (n=6 vessels from 6 animals) (E; 0.5-10 μM). (C, F) maximum change in diameter from each concentration of ML-171 (C) or gp91-dstat (F) relative to control. * Indicates significant difference from control; repeated-measures ANOVA, Bonferroni post-hoc test.

Given the modest dilation induced by Nox1 inhibition, we began to consider whether this ROS generating system was facilitating myogenic constriction by inhibiting a key feedback pathway. Further, we hypothesized that Nox might facilitate myogenic tone by inhibiting Cav3.2, a T-type Ca²⁺ channel that triggers Ca²⁺ release from the RyR on sarcoplasmic reticulum (SR), to activate BK_{Ca} and induce hyperpolarization (11, 39). If correct, inhibitors that block the key mediating steps in this feedback pathway should attenuate the dilatory response induced by Nox1 inhibition. Consistent with our working hypothesis, we found that pre-treating cerebral arteries with paxilline (a BK_{Ca} inhibitor) attenuated the dilation induced by ML-171, a change notable at the lower inhibitor concentrations (Figure 9). A comparison of ML-171-induced dilation, in the presence vs. the absence of paxilline revealed that BK_{Ca} blockade reduced the response by 30-40% (Figure 9). The origins of the BK_{Ca} insensitive component are not currently known.

Nox1 regulation of myogenic constriction via direct interaction with Cav3.2 was tested by repeating the preceding experiment in the presence of Ni²⁺, a selective Cav3.2 inhibitor. Our results show that ML-171 induced dilation was decidedly diminished, with the attenuating effects of 30 μM Ni²⁺ exceeding 50% (10 or 30μM ML-171) when compared to untreated tissues (Figure 10). Cumulatively, these data support our hypothesis that Nox1 regulates myogenic tone in part by altering a key feedback pathway involving Cav3.2 and BK channels.

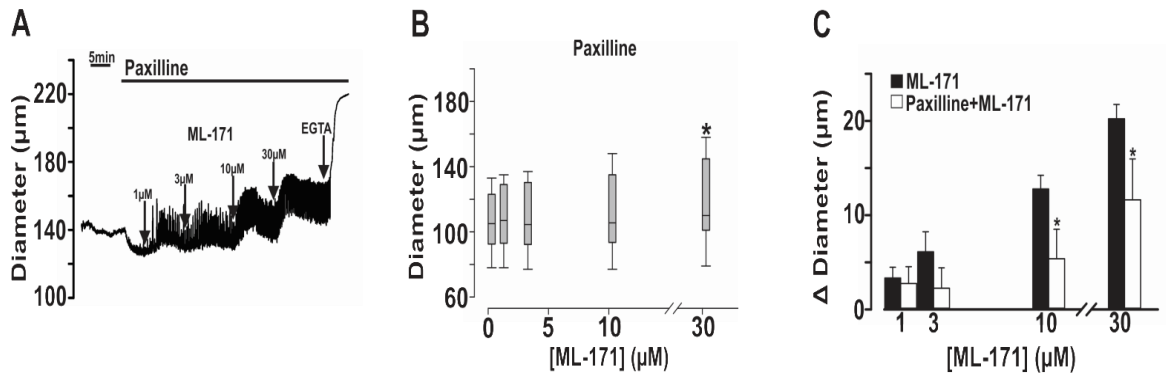


Figure 9: Large-conductance K⁺ (BK) channel blockade and ML171-induced dilation. (A) Representative trace documenting the vasomotor effects of ML-171 in the presence of paxilline (1 µM). (B) Summary data of vessel responsiveness (time averaged, n=6 vessels from 6 animals) to ML-171. Average diameter significantly increases at 10 µM and 30 µM concentrations. (C) Summary data highlighting diameter change to ML-171 in the absence or presence of paxilline (1 µM) (n=6 vessels from 6 animals). * Indicates significant difference from control; repeated measures ANOVA, Bonferroni post-hoc analysis.

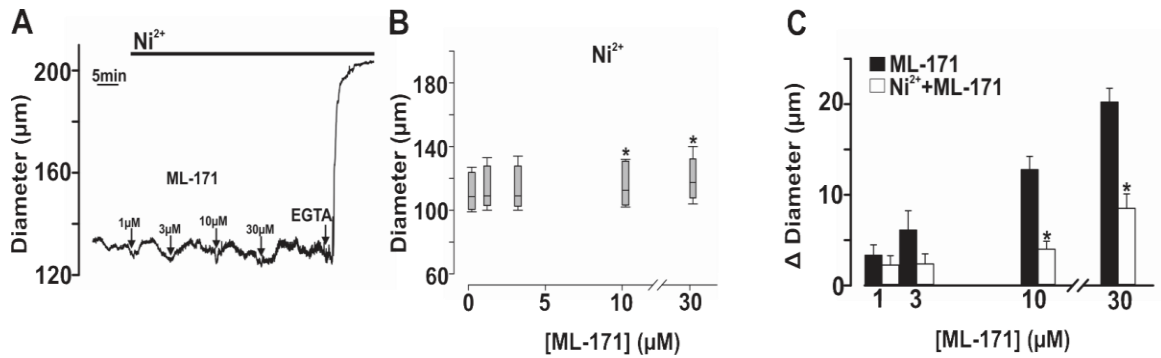


Figure 10: Voltage-gated T-type Calcium Channel (Cav3.2) blockade and ML171-induced dilation. (A) Representative trace documenting the vasomotor effects of ML-171 in the presence of Ni^{2+} (50 µM). (B) Summary data of vessel responsiveness (time averaged, n=6 vessels from 6 animals) to ML-171. (C) Summary data highlighting diameter change to ML-171 in the absence or presence of Ni^{2+} (50 µM) (n=6 vessels from 6 animals). * Indicates significant difference from control; repeated measures ANOVA with Bonferroni post-hoc analysis.

To strengthen the regulatory relationship between Nox1 and Cav3.2, it is important to demonstrate that these two proteins are in close apposition. Immunohistochemistry was first performed on isolated cerebral vascular smooth muscle to confirm Nox1 and Cav3.2 expression (Figure 11). Using fluorophore conjugated secondary antibodies, Nox1 appeared to be broadly distributed in the plasma membrane (Figure 11A), whereas Cav3.2 labeling was decidedly more punctate (Figure 11C). Labeling was absent when primary antibodies were omitted from the experimental protocol (Figure 11B & 11D). Having confirmed expression, we performed the proximity ligation assay (PLA) to assess whether Cav3.2 and Nox1 lie within 40 nm of one another (Figure 12). This assay entails the use of primary antibodies for each protein of interest, which are subsequently bound to selective secondary antibodies attached to synthetic oligonucleotide sequences which hybridized when found in close enough proximity. The hybridized product then undergoes rolling circle amplification via the use of a polymerase; the amplified product is then detected using red fluorophore tagged oligonucleotide sequences. Red fluorescent product was clearly observed at discrete points in the plasma membrane, consistent with Nox1 and Cav3.2 lying in close apposition (Figure 12A-C). Controls were performed by omitting one or both primary antibodies punctate labeling was absent; cell nuclei were visualized with DAPI (Figure 12D-F).

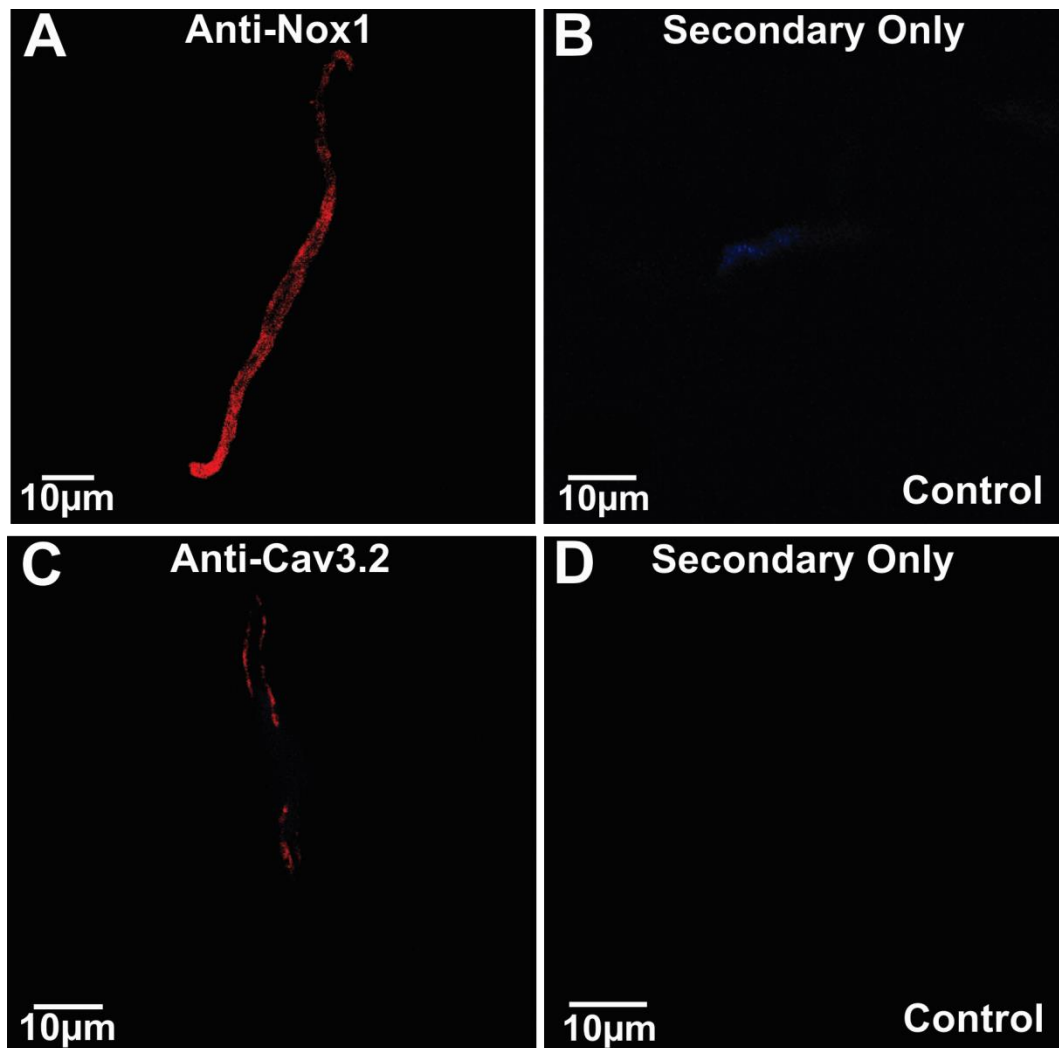


Figure 11: Nox1 and Cav3.2 localization in rat cerebral vascular smooth muscle cells. (A, C) Immunofluorescence images showing smooth muscle cell Nox1 (A) Cav3.2 (C). (B, D) Immunofluorescence images of control experiments containing only secondary antibody.

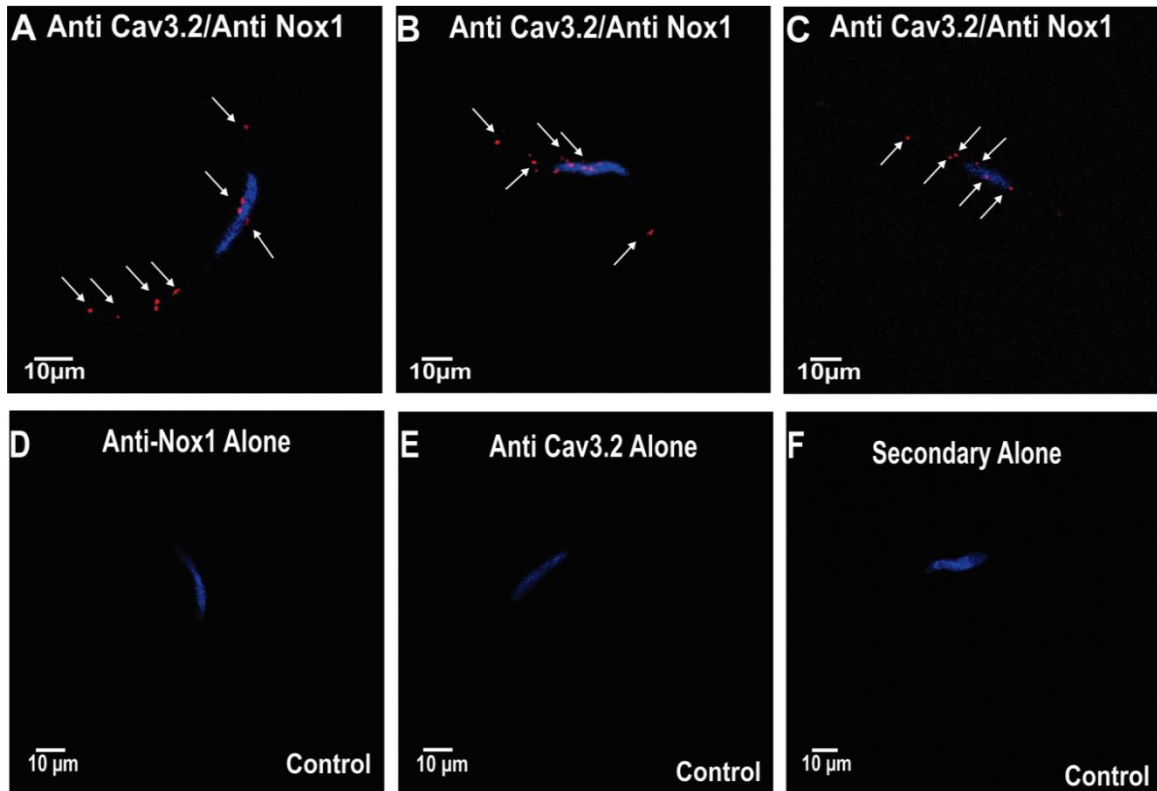


Figure 12: Nox1 and Cav3.2 are found in smooth muscle cells within 40 nm of one another. (A-C) Proximity ligation assay with red dots indicating points of close association of Cav3.2 and Nox1 (≤ 40 nm) with DAPI stained nuclei. (D-F) Control images for proximity ligation assay using only a single primary antibody; either Anti-Nox1 (D), Anti-Cav3.2 (E), or using only the secondary antibody (F).

4 Discussion

This study determined a role for ROS, as generated by Nox, in facilitating myogenic constriction in cerebral arteries. We began our investigation by applying a broad ROS scavenger (TEMPOL) to pressurized cerebral arteries, a perturbation that had no effect on vessel diameter (Figure 5A-5C). We next targeted two prominent ROS generating systems; the first being the mitochondria. In this regard, the inhibitor MitoTEMPO was without effect on vessel tone (Figure 5D-5F). In striking contrast, general Nox inhibition (apocynin) attenuated but did not abolish myogenic constriction in a dose-dependent manner (Figure 6). RT-PCR subsequently confirmed mRNA expression of Nox1 and Nox2 in cerebral arterial smooth muscle cells (Figure 7). Building on these observations, Nox-1 inhibition (ML-171) attenuated myogenic constriction while a Nox2 blocking peptide was without effect (Figure 8). As the attenuation was modest, we subsequently hypothesized that Nox1 was impinging upon a feedback response rather than enhancing the main constrictor mechanism. Of particular note was the ability of extracellular Ca^{2+} influx via $\text{Cav}3.2$, to trigger BK_{Ca} -mediated hyperpolarization and dilation. Consistent with this hypothesis, we showed that ML-171 induced dilation was attenuated in the presence of paxilline or Ni^{2+} , inhibitors of BK and $\text{Cav}3.2$, respectively (Figure 9, Figure 10). Lastly, proximity ligation assay confirmed a close association (~40 nm) between $\text{Cav}3.2$ and Nox1 (Figure 12). Cumulatively, our results are the first to demonstrate that Nox1 facilitates myogenic constriction by inhibiting a key feedback pathway tied to $\text{Cav}3.2$ and the activation of BK channels. The latter hyperpolarizes smooth muscle, diminishing the activity of L-type Ca^{2+} channels and consequently cytosolic $[\text{Ca}^{2+}]$. Our findings highlight the potential of Nox as a therapeutic target in disease states (hypertension and diabetes) in which myogenic reactivity is compromised.

4.1 Background

Regulating the magnitude and distribution of blood flow is critical to vital organs and is governed by the tuning of small resistance vessels. These vessels constrict and dilate in response to various stimuli, one of the most important being intravascular pressure (1-4). The myogenic response refers to the inherent ability of arteries to constrict to a rise in intravascular pressure, a response that provides a base level of tone in key organs such as brain, kidney and heart (5, 13, 42, 43). The myogenic response begins with the

recruitment of a mechanosensor, whose downstream signaling pathway activates a non-selective cation channel and induces arterial depolarization (14). This electrical event increases L-type Ca^{2+} channel activity; the subsequent influx of Ca^{2+} activates MLCK increasing LC20 phosphorylation and crossbridge cycling (4, 5, 10, 13, 14). In addition to this primary mechanism, pressure has been noted to inhibit MLCP via a RhoA-ROK dependant mechanism and promote the formation of filamentous actin (5, 9, 15-20). There are still aspects of myogenic constriction which require clarification, a major one being the identity of the mechansensor. Recent work provides evidence that G-protein coupled receptors may fill this role, including the AT1R (21-23). This receptor, when activated by AngII binding or presumably pressure, induces constriction via a classic G_q coupled pathway. This involves G_q activation of PLC, which subsequently produces IP3 and DAG. The former promotes Ca^{2+} release from the SR while the latter activates protein kinase C (PKC), a serine/threonine kinase that phosphorylates a range of non-selective cation channels (30, 44). The AT1R is linked to additional downstream effectors (21-23), one of interest being the Nox family of enzymes, whose primary function is to produce ROS. While past studies have shown that Nox can target ion channels involved in tone regulation (41, 45, 46), their effect on the myogenic response has not been studied. It is this aspect of cell signaling that will be addressed in this thesis.

4.2 ROS Inhibition and the Myogenic Response

ROS and the deleterious impact of oxidative stress are most often considered in the vascular context of diabetes, hypertension, and atherosclerosis (47-49). Their roles in driving physiological processes are, however, poorly characterized although emerging evidence suggests they may regulate ion channels involved in myogenic constriction (41, 45, 46). It was this aspect of tone development that we first considered by applying a general ROS scavenger (TEMPOL) and monitoring its impact on pressurized vessels. TEMPOL is a SOD mimetic containing a stable free radical which allows this compound to convert superoxide to hydrogen peroxide which is then metabolized to water (50). Our findings highlight that broad-based ROS scavenging had little effect on myogenic tone, as evidenced by the lack of a notable change in vessel diameter in pressurized arteries treated with TEMPOL (Figure 5A-5C). While such findings may suggest ROS do not

play any role in regulating tone, they may alternatively suggest that scavenging ROS from all sources in vascular tissue is too broad of a study, since different sources simultaneously exert different effects on vessel diameter; some constrictor (32, 34-36, 40, 41) and some dilatory (35, 36, 38), removing all of these effects together would have no net effect on tone. This highlights the importance of studying specific ROS generating systems in relation to the myogenic response.

In vascular tissue, the two dominant systems of ROS generation are Nox and the mitochondria (32, 34, 45), the latter of which we targeted with the ROS scavenger mitoTEMPO, an agent comprised of the ROS scavenger TEMPO which has a similar mechanism of action to TEMPOL, combined with the lipophilic cation triphenylphosphonium (TPP⁺) allowing it to target the mitochondria specifically (51). Akin to TEMPOL, findings show that mitoTEMPO had no substantive effect on vessel diameter when applied at concentrations that varied from 1-30 μ M. (Figure 5D-5F). This observation contrasts the work of Chaplin and colleagues (45) whose findings suggest that mitochondrial ROS generation upregulates L-type Ca²⁺ channel activity, leading to vessel constriction (45). The notable difference between past and present findings may reflect how the vessel was precontracted (by pressure or agonist) and whether the stimulus initiated ROS production (40, 45, 46). In light of these null findings, this study shifted its attention to Nox.

4.3 Nox Inhibition Dilates Pressurized Arteries

The Nox family of enzymes are comprised of seven isoforms and in vascular tissue Nox1, Nox2, Nox4, and Nox5 dominate (36, 38). All isoforms consist of a catalytic membrane-bound complex comprised of six-transmembrane α -helices bound to two heme groups and an FAD molecule. Nox1 and Nox2 are of particular importance to this study as they localize to the plasma membrane (35, 36, 38, 52). When active, they are comprised of three universal subunits (p22phox, p47phox and Rac) and one isoform specific subunit NoxA1 (Nox1) and p67phox (Nox2) (35, 36). We began our investigation of Nox-generated ROS by applying apocynin, a broad spectrum inhibitor which retains reasonable target specificity when used at concentrations at or below 300

μM (53-55). We intriguingly observed a concentration-dependent dilation of pressurized vessels which displayed a transient and a sustained component (Figure 6). While the mechanism of action has yet to be fully elucidated, it is possible that apocynin diminishes Nox inhibition by interfering with the translocation of the cytosolic subunits to the membrane (53-55). With these findings indicating a role for Nox-generated ROS in myogenic tone development, we next sought to determine which isoform was specifically involved. Quantitative real-time PCR analysis revealed that Nox1 and Nox2 mRNA were expressed in cerebral arterial smooth muscle cells and as such, both would have to be investigated at the functional level (34-36, 38) (Figure 7). In this regard, we first targeted Nox1 by applying ML-171 to pressurized arteries. While this compound's mechanism of action is not well characterized, it has demonstrated some specificity for the Nox1 membrane subunit over any other isoforms or subunits (56-58). Our findings mirrored those of apocynin, in that ML-171 induced a concentration-dependent dilation which retained a transient and sustained component (Figure 8A-8C). In sharp contrast, the Nox2 inhibitor (gp91-dstat) which interferes with p47 binding to the Nox2 membrane complex (57-59), had no notable impact on myogenic tone development (Figure 8D-8F). Cumulatively, the preceding work indicates that Nox1 rather than Nox2 is the isoform responsible for facilitating the myogenic response (Figure 8).

The preceding dilatory response to Nox inhibition was more modest and generally not what was expected if ROS was targeting L-type Ca^{2+} channels, a key enabler of myogenic constriction. (40, 42, 43, 45). This observation, lead us to consider whether Nox-derived ROS was directed towards the modulation of a feedback pathway (10, 11, 32). In this regard, Nox1 is known to associate with caveolae (41, 44) as does $\text{Ca}_v3.2$, a T-type Ca^{2+} channel (10, 11, 39). Previous work has shown that Ca^{2+} entry via $\text{Ca}_v3.2$ can trigger the cytosolic gate of RyR eliciting discrete events called Ca^{2+} sparks (10, 11, 39, 60, 61). These sparks in turn transiently activate BK_{Ca} producing spontaneous transient outward currents (STOC) that hyperpolarize the cell, reduce L-type Ca^{2+} channel activity and attenuate constriction (10, 11, 32, 60, 61). Given the modest nature of dilation observed with Nox1 inhibition, and published work showing that the $\text{Ca}_v3.2$ channels contain an oxidation site at histidine 191 (H191) (62), we rationalized that Nox1

facilitates myogenic constriction by inhibiting Cav3.2 and moderating BK_{Ca}-mediated feedback.

4.4 Nox1 Impacts BK-mediated Feedback

If Nox1 facilitates myogenic constriction by lowering BK_{Ca}-mediated feedback, then ML-171 induced dilation should be attenuated when key components of this transduction pathway are blocked. To test this hypothesis, cerebral arteries were pressurized to 60 mmHg and the dilatory response to ML-171 monitored in the absence and presence of the BK channel inhibitor, paxilline. Paxilline (1 μ M) markedly attenuated the dilation induced by ML-171 at concentrations < 10 μ M. Upon increasing ML-171 concentration to 30 μ M, paxilline attenuated the dilatory response by 30% (Figure 9). These data generally support the idea that Nox1 affects BK_{Ca}-mediated feedback. To address whether Cav3.2 is targeted by Nox1 in this feedback pathway, the preceding ML-171 experiments were repeated in the absence and presence of Ni²⁺ (50 μ M). In the presence of this Cav3.2 inhibitor, application of ML-171 at concentrations <10 μ M was greatly diminished, while the dilatory response of \geq 10 μ M ML-171 was attenuated by over 50% (Figure 10). These findings support our view that Nox1 may indeed facilitate myogenic constriction by moderating BK_{Ca}-mediated feedback via Cav3.2 inhibition. Note, recent mechanistic work has shown that Cav3.2 is subject to inhibition via ROS oxidation at the H191 residue (62). While Nox1 regulation of Cav3.2 is functionally important, this ROS generating enzyme likely has other downstream targets as neither paxilline nor Ni²⁺ completely blocked ML-171 induced dilation. This could be an important avenue for future study but is beyond the scope of the present work.

4.5 Nox1 Localization with Cav3.2

For Nox1-generated ROS to interact with Cav3.2, it is clear that the two proteins must reside in close apposition with one another. To visualize this close association, we undertook a set of immunolabeling experiments. First, traditional immunohistochemistry approaches were used to visualize the distribution pattern of Nox1 and Cav3.2 in vascular smooth muscle (Figure 11). Confocal microscopy employing fluorophore-conjugated secondary antibodies confirmed that Nox1 was broadly distributed along vascular smooth

muscle cells while Cav3.2 was expressed in more discrete regions along the plasma membrane, consistent with published work (10, 11, 34-38, 41) (Figure 11). A more broad distribution of Nox1 in smooth muscle cells supports the idea that it has additional downstream targets, which would explain why Cav3.2 inhibition did not entirely abolish ML-171-induced dilation. Subsequently, PLA, a technology that extends traditional immunoassays, was employed and synthetic oligonucleotide probes were used which hybridize when found ≤ 40 nm to both Nox1 and Cav3.2. Hybridized products were amplified with polymerase and visualized with red fluorophore conjugated oligonucleotides, appearing as red spots at discrete points along isolated cells. (Figure 12) These results align with previous work which show that both Nox1 (34-36, 38, 45, 46), and Cav3.2 (10, 11, 39, 41) are found at plasma membrane caveolae, thus providing evidence that Nox-generated ROS are able to reach and interact with Cav3.2 (Figure 13).

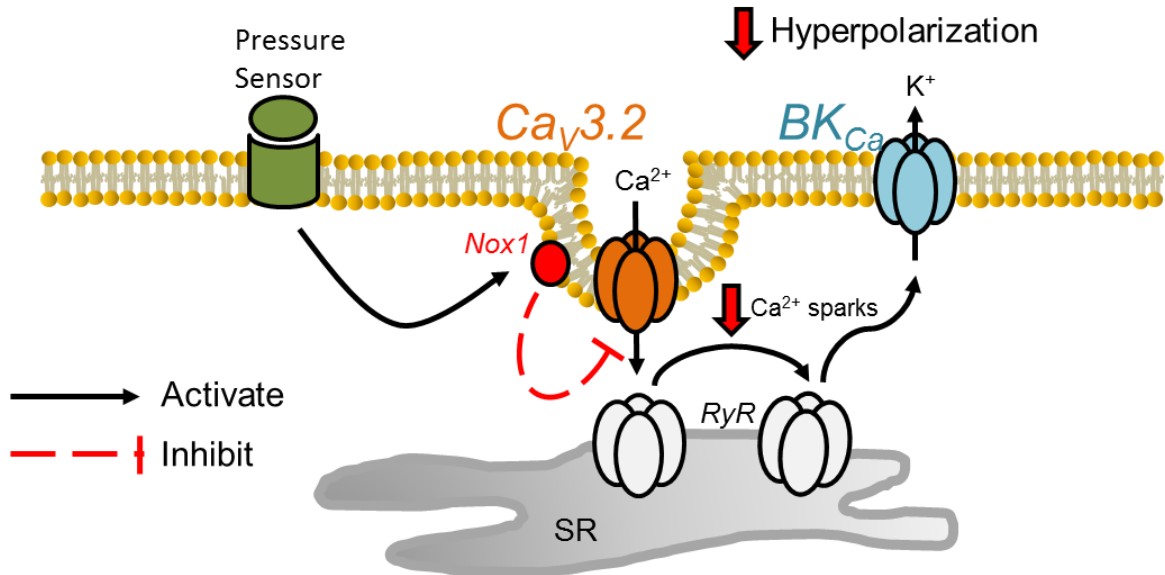


Figure 13: Proposed Mechanism of Action of Nox1 Regulation of Myogenic Constriction. Nox1 facilitates constriction by moderating BK_{Ca}-induced negative feedback. Intravascular pressure activates Nox1, which subsequently inhibits Ca_v3.2, lowering Ca²⁺ spark production and subsequent hyperpolarizing STOCs from BK_{Ca}, thereby increasing the open-probability of L-type Ca²⁺ channels, the primary source of Ca²⁺ required for constriction.

4.6 Limitations

While apocynin is widely viewed as a Nox inhibitor (53-55), it has been suggested that in vascular smooth muscle it is a more potent ROS scavenger (63). This was an important consideration as it could indicate that the observed apocynin effects might be due to broad-based ROS scavenging rather than specific inhibition of Nox. Two steps were taken to address this concern, the first being that apocynin concentrations did not exceed 300 μM , the point at which broader ROS scavenging effects are typically observed (63). Second, we examined the effects of a broad-based ROS scavenger (TEMPOL) and found that it had no substantive effect on myogenic tone development. This lies in contrast to apocynin application which elicited a dose dependent vasodilation. Target specificity has also been a concern with ML-171, as previous work suggests that in addition to inhibiting Nox1, it can target Nox2 (56-58). Two important measures were again taken to address the compound's specificity. First, ML-171 concentrations were kept $\leq 30 \mu\text{M}$, a dose that has limited impact on the Nox2 ROS generating system (56). Second, we examined the effects of a Nox2 peptide inhibitor (gp91-dstat) and found no notable effect on myogenic tone development. This functional phenotype is different from the concentration-dependent dilation induced by ML-171.

It should be clearly noted that this study specifically focused on Nox1 and Nox2 as these ROS generating enzymes are present in the plasma membrane (35, 36, 38, 52) and regulate Ca^{2+} channels involved in myogenic tone development (4, 10, 11, 39). Nox4 and Nox5 on the other hand, do not adhere to this criteria, thus they are unlikely to impact ion channels involved in vasomotor control (34-36, 38). Further to this point, there is no evidence that Nox4 can modulate tone, except perhaps in disease states that acutely affect brain blood flow (64). The physiological importance of Nox5 is difficult to assess in rodent, as expression is sparse in vascular smooth muscle (35, 36).

4.7 Future Directions

To strengthen the relationship between Nox1, $\text{Cav}3.2$, and BK_{Ca} -mediated feedback, it would be valuable to directly assess the effect of Nox1 inhibition on these key ion channels by undertaking patch-clamp electrophysiology. Of particular note would be

measurements of Ca^{2+} sparks and STOCs, in the presence and absence of ML-171, to directly link Nox1 regulation to $\text{Cav}3.2$ or BK_{Ca} activity. There is also considerable value in directly measuring Nox expression and activity using western blot techniques or ROS sensitive dyes, respectively. Lastly, the dilatory phenotypes induced by pharmacological Nox inhibitors in pressurized vessels should be verified in knock-out (KO) animal models. It would be of particularly value to compare the myogenic response in resistance arteries of Nox1 knockout animals to wild-type controls.

To build upon the present study, two critical mechanisms regarding the ability of Nox to regulate myogenic tone may be further studied. First it is important to mechanistically resolve the component of ML-171-induced dilation insensitive to paxilline or Ni^{2+} . While data is limited, Nox1-generated ROS may be targeting more than one feedback mechanism (61). One mechanism of note involves the multiple K_v channels that are expressed in vascular smooth muscle cells (61). Second, the mechanism by which Nox1 can affect $\text{Cav}3.2$ should be determined. Previous work suggests that Nox-derived ROS affects vascular Voltage-gated Ca^{2+} channels (VGCC) via a mechanism dependent on Protein Kinase C (PKC) (65-70). ROS has been shown to activate PKC (68) and consequently neighboring L-type Ca^{2+} channels (66-70). Pressure myography, electrophysiology and immunofluorescence techniques may be applied to determine if a similar mechanism links Nox1 and $\text{Cav}3.2$. Alternatively, Orestes and colleagues have shown that ROS may directly oxidize the H191 site of $\text{Cav}3.2$ resulting in channel inhibition (62). While intriguing, these findings are currently limited to neural $\text{Cav}3.2$ (62) and replicating this work in vascular tissue would be of value to the myogenic field of study.

4.8 Summary

The findings of this study support the idea that Nox1-generated ROS plays a role in facilitating myogenic constriction in cerebral resistance arteries via inhibition of BK_{Ca} -induced negative feedback. We provide evidence that Nox1 is in close proximity to, and suppresses $\text{Cav}3.2$ channel activity, reducing BK_{Ca} -induced hyperpolarization, thereby increasing the open-probability of L-type Ca^{2+} channels, the main source of Ca^{2+} required for constriction. This study is the first to provide evidence that Nox1-generated ROS

facilitates constriction by inhibiting a feedback pathway rather than by enhancing a main constrictor mechanism. This newly proposed mechanism of tone regulation has potential to contribute to combating the excessive constriction often observed in vascular disease states such as hypertension or diabetes.

References

1. Garcia-Roldan JL, Bevan JA. Flow-Induced Constriction and Dilation of Cerebral Resistance Arteries. *Circulation Research*. 1990; 66:1445–1448.
2. Bevan JA, Garcia-Roldan JL, Joyce EH. Resistance Artery Tone is Influenced Independently by Pressure and by Flow. *Blood Vessels*. 1990; 27:202–207
3. Filosa JA, Bonev AD, Straub SV, Meredith AL, Wilkerson MK, Aldrich RW, Nelson MT. Local Potassium Signaling Couples Neuronal Activity to Vasodilation in the Brain. *Nature Neuroscience*. 2006; 9:1397–1403.
4. Knot HJ, Nelson MT. Regulation of Arterial Diameter and Wall $[Ca^{2+}]$ in Cerebral Arteries of Rat by Membrane Potential and Intravascular Pressure. *The Journal of Physiology*. 1998; 508(1):199–209.
5. Cole WC, Welsh DG. Role of Myosin Light Chain Kinase and Myosin Light Chain Phosphatase in the Resistance Arterial Myogenic Response to Intravascular Pressure. *Archives of Biochemistry and Biophysics*. 2011; 510(2), 160–173
6. Mulvany MJ and Aalkjaer C. Structure and Function of Small Arteries. *Physiological Reviews*. 1990; 70(4): 921-961
7. Wölfle SE, Chaston DJ, Goto K, Sandow SL, Edwards FR, Hill CE. Non-Linear Relationship Between Hyperpolarisation and Relaxation Enables Long Distance Propagation of Vasodilatation. *The Journal of Physiology*. 2011; 589(10):2607-2623.
8. Walsh, MP, Cole WC. The Role of Actin Filament Dynamics in the Myogenic Response of Cerebral Resistance Arteries. *Journal of Cerebral Blood Flow & Metabolism* 2013; 33(1) 1–12.
9. Gunst SJ, Zhang W. Actin Cytoskeletal Dynamics in Smooth Muscle: a New Paradigm for the Regulation of Smooth Muscle Contraction. *American Journal of Physiology - Cell Physiology*. 2008; 295(3):C576-C587.

10. El-Rahman RR, Harraz OF, Brett SE, Anfinogenova Y, Mufti RE, Goldman D, Welsh DG. Identification of L- and t-type Ca²⁺ Channels in Rat Cerebral Arteries: Role in Myogenic Tone Development. *American Journal of Physiology- Heart and Circulatory Physiology*. 2012; 304(1):H58-H71.
11. Harraz OF, Abd El-Rahman RR, Bigdely-Shamloo K, Wilson SM, Brett SE, Romero M, Gonzales AL, Earley S, Vigmond EJ, Nygren A, Menon BK, Mufti RE, Watson T, Starreveld Y, Furstenhaupt T, Muellerleile PR, Kurjiaka DT, Kyle BD, Braun AP, Welsh DG. CaV3.2 Channels and the Induction of Negative Feedback in Cerebral Arteries. *Circulation research*. 2014; 115(7):650-661.
12. Ito M, Nakano T, Erdodi F, Hartshorne DJ. Myosin Phosphatase: Structure, Regulation and Function. *Molecular and Cellular Biochemistry*. 2004; 259(1-2):197-209.
13. Bayliss WM. On the Local Reactions of the Arterial Wall to Changes of Internal Pressure. *The Journal of Physiology*, 1902; 28: 220–223.
14. Welsh DG, Morielli AD, Nelson MT, Brayden JE. Transient Receptor Potential Channels Regulate Myogenic Tone of Resistance Arteries. *Circulation Research*. 2002; 90:248-250.
15. Johnson RP, El-Yazbi AF, Takeya K, Walsh EJ, Walsh MP, Cole WC. Ca²⁺ Sensitization via Phosphorylation of Myosin Phosphatase Targeting Subunit at Threonine-855 by Rho Kinase Contributes to the Arterial Myogenic Response. *The Journal of Physiology*. 2009; 587(11):2537-2553.
16. Moreno-Domínguez A, Colinas O, El-Yazbi A, Walsh EJ, Hill MA, Walsh MP, Cole WC. Ca²⁺ Sensitization due to Myosin Light Chain Phosphatase Inhibition and Cytoskeletal Reorganization in the Myogenic Response of Skeletal Muscle Resistance Arteries. *The Journal of Physiology*. 2013; 591(5):1235-1250.
17. El-Yazbi AF, Johnson RP, Walsh EJ, Takeya K, Walsh MP, Cole WC. Pressure-Dependent Contribution of Rho Kinase-Mediated Calcium Sensitization in Serotonin-

Evoked vasoconstriction of rat cerebral arteries. *The Journal of Physiology*. 2010; 588(10):1747-1762.

19. Wu Y, Gunst SJ. Vasodilator-Stimulated Phosphoprotein (VASP) Regulates Actin Polymerization and Contraction in Airway Smooth Muscle by a Vinculin-Dependent Mechanism. *Journal of Biological Chemistry*. 2015; 290(18):11403-11416.

20. Zhang W, Huang Y, Gunst SJ. The Small GTPase RhoA Regulates the Contraction of Smooth Muscle Tissues by Catalyzing the Assembly of Cytoskeletal Signaling Complexes at Membrane Adhesion Sites. *Journal of Biological Chemistry*. 2012; 287(41):33996-34008.

21. Schnitzler MM, Storch U, Meibers S, Nurwakagari P, Breit A, Essin K, Gollasch M, Gudermann T. Gq-Coupled Receptors as Mechanosensors Mediating Myogenic Vasoconstriction. *The EMBO Journal*. 2008; 27(23):3092-3103.

22. Schleifenbaum J, Kassmann M, Szijártó IA, Hercule HC, Tano JY, Weinert S, Heidenreich M, Pathan AR, Anistan YM, Alenina N, Rusch NJ, Bader M, Jentsch TJ, Gollasch M. Stretch Activation of Angiotensin II Type 1a Receptors Contributes to the Myogenic Response of Mouse Mesenteric and Renal Arteries. *Circulation Research*. 2014; 115:263-272.

23. Pires PW, Ko EA, Pritchard HAT, Rudokas M, Yamasaki E, Earley S. The Angiotensin II Receptor Type 1b is the Primary Sensor of Intraluminal Pressure in Cerebral Artery Smooth Muscle Cells. *The Journal of Physiology*. 2017; 595(14):4735-4753

24. Martinez-Lemus LA, Wu X, Wilson E, Hill MA, Davis GE, Davis MJ, Meininger GA. Integrins as Unique Receptors for Vascular Control. *Journal of Vascular Research*. 2003; 40:211-233.

25. Martinez-Lemus LA, Crow T, Davis MJ, Meininger GA. Alpha5beta1- and Alpha5beta3-integrin Blockade Inhibits Myogenic Constriction of Skeletal Muscle

Resistance Arterioles. *Am Journal of Physiology-Heart and Circulatory Physiology*. 2005; 289(1):H322-H329.

26. Davis MJ, Wu X, Nurkiewicz TR, Kawasaki J, Davis GE, Hill MA, Meininger GA. Integrins and Mechanotransduction of the Vascular Myogenic Response. *American Journal of Physiology-Heart and Circulatory Physiology*. 2001; 280(4):H1427-H1433.

27. Lohse MJ, Maiellaro I, Calebiro D. Kinetics and mechanism of G Protein-Coupled Receptor Activation. *Current Opinion in Cell Biology*. 2014; 27:87-93.

28. Rosenbaum DM, Rasmussen SGF, Kobilka BK. The Structure and Function of G-Protein-Coupled Receptors. *Nature*. 2009; 459(7245):356-363.

29. Fredriksson R, Lagerström MC, Lundin LG, Schiöth HB. The G-protein-Coupled Receptors in the Human Genome Form Five Main Families. Phylogenetic Analysis, Paralogon groups, and fingerprints. *Molecular Pharmacology*. 2003; 63(6):1256-1272.

30. Nguyen Dinh Cat A, Touyz RM. Cell Signaling of Angiotensin II on Vascular Tone: Novel Mechanisms. *Current Hypertension Reports*. 2011; 13(2): 122-128.

31. De Silva TM, Faraci FM. Effects of Angiotensin II on the Cerebral Circulation: Role of Oxidative Stress. *Frontiers in Physiology*. 2012; 3:484.

32. Nguyen Dinh Cat A, Montezano AC, Burger D, Touyz RM. Angiotensin II, NADPH Oxidase, and Redox Signaling in the Vasculature. *Antioxidants & Redox Signaling*. 2013; 19(10):1110-1120.

33. Seko T, Ito M, Kureishi Y, Okamoto R, Moriki N, Onishi K, Isaka N, Hartshorne DJ, Nakano T. Activation of RhoA and Inhibition of Myosin Phosphatase as Important Components in Hypertension in Vascular Smooth Muscle. *Circulation Research*. 2003; 92(4):411-418.

34. Drummond GR, Selemidis S, Griendling KK, Sobey CG. Combating Oxidative Stress in Vascular Disease: NADPH Oxidases as Therapeutic Targets. *Nature Reviews Drug Discovery*. 2011; 10(6):453-471.

35. Lassègue B, Griendling KK. NADPH Oxidases: Functions and Pathologies in the Vasculature. *Arteriosclerosis, Thrombosis, and Vascular Biology*. 2010; 30(4):653-661.
36. Lassègue B, San Martín A, Griendling KK. Biochemistry, Physiology and Pathophysiology of NADPH Oxidases in the Cardiovascular System. *Circulation Research*. 2012; 110(10):1364-1390.
37. Bokoch GM, Diebold BA. Current Molecular Models for NADPH Oxidase Regulation by Rac GTPase. *Blood*. 2002; 100(8):2692-2696.
38. Lassègue B, Clempus RE. Vascular NAD(P)H Oxidases: Specific Features, Expression, and Regulation. *American Journal of Physiology-Regulatory, Integrative and Comparative Physiology*. 2003; 285(2):R277-R297.
39. Hashad AM, Mazumdar N, Romero M, Nygren A, Bigdely-Shamloo K, Harraz OF, Puglisi JL, Vigmond EJ, Wilson SM, Welsh DG. Interplay Among Distinct Ca²⁺ Conductances Drives Ca²⁺ Sparks/Spontaneous Transient Outward Currents in Rat Cerebral Arteries. *The Journal of Physiology*. 2017; 595(4):1111-1126.
40. Amberg GC, Earley S, Glapa SA. Local Regulation of Arterial L-Type Calcium Channels by Reactive Oxygen Species. *Circulation Research*. 2010; 107(8):1002-1010.
41. Hashad AM, Sancho M, Brett SE, Welsh DG. Reactive Oxygen Species Mediate the Suppression of Arterial Smooth Muscle T-type Ca²⁺ Channels by Angiotensin II. *Scientific Reports*. 2018; 8:3445.
42. Davis MJ. Perspective: Physiological Role(s) of the Vascular Myogenic Response. *Microcirculation*. 2012; 19(2):99-114.
43. Schubert R, Mulvany MJ. The Myogenic Response: Established Facts and Attractive Hypotheses. *Clinical Science*. 1999; 96(4):313-326.
44. Osol G, Laher I, Cipolla M. Protein Kinase C Modulates Basal Myogenic Tone in Resistance Arteries from the Cerebral Circulation. *Circulation Research*. 1991; 68(2):359-67.

45. Chaplin NL, Nieves-Cintrón M, Fresquez AM, Navedo MF, Amberg GC. Arterial Smooth Muscle Mitochondria Amplify Hydrogen Peroxide Microdomains Functionally Coupled to L-Type Calcium Channels. *Circulation Research*. 2015; 117(12):1013-1023.
46. Chaplin NL, Amberg GC. Hydrogen Peroxide Mediates Oxidant-Dependent Stimulation of Arterial Smooth Muscle L-type Calcium Channels. *American Journal of Physiology-Cell Physiology*. 2012; 302(9):C1382-C1393.
47. Battered LD, Springall DR, Chester AH, Evans TJ, Standfield EN, Parums DV, Yacoub MH, Polak JM. Inducible Nitric Oxide Synthase is Present Within Human Atherosclerotic Lesions and Promotes the Formation and Activity of Peroxynitrite. *Laboratory Investigation*. 1996; 75(1): 77-85
48. Grunfeld S, Hamilton CA, Mesaros S, McClain SW, Dominiczak AF, Bohr DF, Malinski T. Role of Superoxide in the Depressed Nitric Oxide Production by the Endothelium of Genetically Hypertensive Rats. *Hypertension*. 1995; 26(6):854-857
49. Kamata K, Kobayashi T. Changes in Superoxide Dismutase mRNA Expression by Streptozotocin-Induced Diabetes. *British Journal of Pharmacology*. 1996; 119(3): 583-589
50. Wilcox CS, Pearlman A. Chemistry and Antihypertensive Effects of TEMPOL and Other Nitroxides. *Pharmacological Reviews*. 2008; 60(4):418-469.
51. Du K, Farhood A, Jaeschke H. Mitochondria-Targeted Antioxidant Mito-Tempo Protects against Acetaminophen Hepatotoxicity. *Archives of Toxicology*. 2017; 91(2):761-773.
52. Hilenski LL, Clempus RE, Quinn MT, Lambeth JD, Griendling KK. Distinct Subcellular Localizations of Nox1 and Nox4 in Vascular Smooth Muscle Cells. *Arteriosclerosis, Thrombosis, and Vascular Biology*. 2004; 24(4):677-683.
53. Stefanska J, Pawliczak R. Apocynin: Molecular Aptitudes. *Mediators of Inflammation*. 2008; 2008:106507.

54. Barbieri SS, Cavalca V, Eligini S, Brambilla M, Caiani A, Tremoli E, Colli S. Apocynin Prevents Cyclooxygenase 2 Expression in Human Monocytes Through NADPH Oxidase and Glutathione Redox-Dependent Mechanisms. *Free Radical Biology and Medicine*. 2004; 37(2):156-165.
55. Peters EA, Hiltermann JT, Stolk J. Effect of Apocynin on Ozone-Induced Airway Hyperresponsiveness to Methacholine in Asthmatics. *Free Radical Biology and Medicine*. 2001; 31(11):1442-1447.
56. Gianni D, Taulet N, Zhang H, DerMardirossian C, Kister J, Martinez L, Roush WR, Brown SJ, Bokoch GM, Rosen H. A Novel and Specific NADPH Oxidase-1 (Nox1) Small-Molecule Inhibitor Blocks the Formation of Functional Invadopodia in Human Colon Cancer Cells. *ACS Chemical Biology*. 2010; 5(10):981-993.
57. Cifuentes-Pagano E, Meijles DN, Pagano PJ. The Quest for Selective Nox Inhibitors and Therapeutics: Challenges, Triumphs and Pitfalls. *Antioxidants & Redox Signaling*. 2014; 20(17):2741-2754.
58. Altenhöfer S, Radermacher KA, Kleikers PWM, Wingler K, Schmidt HHHW. Evolution of NADPH Oxidase Inhibitors: Selectivity and Mechanisms for Target Engagement. *Antioxidants & Redox Signaling*. 2015; 23(5):406-427.
59. Csányi G, Cifuentes-Pagano E, Al Ghouleh I, Ranayhossaini DJ, Egaña L, Lopes LR, Jackson HM, Kelley EE, Pagano PJ. Nox2 B-loop Peptide, Nox2ds, Specifically Inhibits Nox2 Oxidase. *Free Radical Biology & Medicine*. 2011; 51(6):1116-1125.
60. Trebak M, Ginnan R, Singer HA, Jourdain D. Interplay Between Calcium and Reactive Oxygen/Nitrogen Species: An Essential Paradigm for Vascular Smooth Muscle Signaling. *Antioxidants & Redox Signaling*. 2010; 12(5):657-674.
61. Thorneloe KS, Nelson MT. Ion Channels in Smooth Muscle: Regulators of Intracellular Calcium and Contractility. *Canadian Journal of Physiology and Pharmacology*. 2005; 83(3):215-242.

62. Orestes P, Bojadzic D, Lee J, Leach E, Salajegheh R, Digruccio MR, Nelson MT, Todorovic SM. Free Radical Signalling Underlies Inhibition of CaV3.2 T-type Calcium Channels by Nitrous Oxide in the Pain Pathway. *The Journal of Physiology*. 2011; 589(1):135–148.
63. Heumüller S, Wind S, Barbosa-Sicard E, Schmidt HH, Busse R, Schröder K, Brandes RP. Apocynin is Not an Inhibitor of Vascular NADPH Oxidases but an Antioxidant. *Hypertension*. 2008; 51(2):211-217.
64. Kleinschnitz C, Grund H, Wingler K, Armitage ME, Jones E, Mittal M, Barit D, Schwarz T, Geis C, Kraft P, Barthel K, Schuhmann MK, Herrmann AM, Meuth SG, Stoll G, Meurer S, Schrewe A, Becker L, Gailus-Durner V, Fuchs H, Klopstock T, de Angelis MH, Jandeleit-Dahm K, Shah AM, Weissmann N, Schmidt HH. Post-Stroke Inhibition of Induced NADPH Oxidase Type 4 Prevents Oxidative Stress and Neurodegeneration. *PLoS Biology*. 2010; 8(9):e1000479.
65. Chaplin NL, Amberg GC. Stimulation of Arterial Smooth Muscle L-type Calcium Channels by Hydrogen Peroxide Requires Protein Kinase C. *Channels*. 2012; 6(5):385-389.
66. Gupte SA, Kaminski PM, George S, Kouznestova L, Olson SC, Mathew R, Hintze TH, Wolin MS. Peroxide Generation by p47^{phox}-Src Activation of Nox2 has a Key Role in Protein Kinase C-Induced Arterial Smooth Muscle Contraction. *American Journal of Physiology - Heart and Circulatory Physiology*. 2009; 296(4):H1048-H1057.
67. Feissner RF, Skalska J, Gaum WE, Sheu S-S. Crosstalk Signaling Between Mitochondrial Ca²⁺ and ROS. *Frontiers in Bioscience: a journal and virtual library*. 2009; 14:1197-1218.
68. Hidalgo C, Donoso P. Crosstalk Between Calcium and Redox Signaling: from Molecular Mechanisms to Health Implications. *Antioxidants & Redox Signaling*. 2008; 10(7):1275-1312.

69. Terada LS. Specificity in Reactive Oxidant Signaling: Think Globally, Act Locally. *The Journal of Cell Biology*. 2006; 174(5):615-623.
70. Knapp LT, Klann E. Superoxide-Induced Stimulation of Protein Kinase C via Thiol Modification and Modulation of Zinc Content. *Journal of Biological Chemistry*. 2000; 275(31):24136-24145

Appendices

Appendix 14: Animal Use Protocol Approval



AUP Number: 2015-060

PI Name: Welsh, Donald

AUP Title: Function and Regulation of T-type Ca²⁺ Channels in the Cerebral Circulation

Official Notification of AUS Approval: A MODIFICATION to Animal Use Protocol 2015-060 has been approved.

The holder of this Animal Use Protocol is responsible to ensure that all associated safety components (biosafety, radiation safety, general laboratory safety) comply with institutional safety standards and have received all necessary approvals. Please consult directly with your institutional safety officers.

Submitted by: Copeman, Laura
on behalf of the Animal Care Committee

The University of Western Ontario
Animal Use Subcommittee / University Council on Animal Care

Curriculum Vitae

Name Neil Mazumdar

Education

Master of Science 2015-2018

Physiology and Pharmacology

University of Western Ontario London, Ontario, Canada

Bachelor of Health Sciences 2010-2014

Major in Biomedical Sciences

University of Calgary Calgary, Alberta, Canada

Awards and Scholarships

University of Calgary Entrance Scholarship 2010

NSERC Summer Studentship 2014

Jason Lang Scholarship 2014

Publications and Presentations

Hashad, A. M., Mazumdar, N., Romero, M., Nygren, A., Bigdely-Shamloo, K., Harraz, O. F., Puglisi, J. L., Vigmond, E. J., Wilson, S. M. and Welsh, D. G. (2017), Interplay among distinct Ca²⁺ conductances drives Ca²⁺ sparks/spontaneous transient outward currents in rat cerebral arteries. *J Physiol*, 595: 1111–1126.

Mufti R. E., Zechariah A., Sancho M., Mazumdar N., E. Brett S. E., Welsh D. G. (2015). Implications of $\alpha\beta3$ Integrin Signaling in the Regulation of Ca²⁺ Waves and Myogenic Tone in Cerebral Arteries. *Arteriosclerosis, Thrombosis, and Vascular Biology*. 115(305619)

Neil Mazumdar N., Hanna Jalali H., Ahmed Hashad A. M., Visser F*, Welsh D. G. The Role of NADPH Oxidase in Regulating Cerebral Vascular Myogenic Tone. *Experimental Biology*, 2017

Neil Mazumdar N., Hanna Jalali H., Ahmed Hashad A. M., Visser F*, Welsh D. G. The Role of NADPH Oxidase in Regulating Cerebral Vascular Myogenic Tone. *Robarts Research Retreat*, 2017

Hashad A. M., Mazumdar N., Harraz O. F., Welsh D. G. (2014). The role of Ca²⁺ influx pathways in voltage-dependent STOC production. *The Journal of the Federation of American Societies for Experimental Biology. International Symposium on Resistance Arteries*, 2015-11-07